



UNIVERSIDAD DE INVESTIGACIÓN DE TECNOLOGÍA EXPERIMENTAL YACHAY

Escuela de Ciencias Físicas y Nanotecnología

TÍTULO: Viscosity Analysis of Clay-Carbon Nanotubes Composites as Potential Drilling Muds

Trabajo de integración curricular presentado como requisito para
la obtención del título de Física

Autor:

Quilumba Dutan Verónica Alexandra

Tutor:

Ph.D Chacón Torres Julio

Urcuquí, agosto 2019

Urcuquí, 21 de agosto de 2019

SECRETARÍA GENERAL
(Vicerrectorado Académico/Cancillería)
ESCUELA DE CIENCIAS FÍSICAS Y NANOTECNOLOGÍA
CARRERA DE FÍSICA
ACTA DE DEFENSA No. UITEY-PHY-2019-00008-AD

En la ciudad de San Miguel de Urcuquí, Provincia de Imbabura, a los 21 días del mes de agosto de 2019, a las 08:30 horas, en el Aula Sala Capitular de la Universidad de Investigación de Tecnología Experimental Yachay y ante el Tribunal Calificador, integrado por los docentes:

Presidente Tribunal de Defensa Dr. ZAMORA LEDEZMA, CAMILO Ph.D.
Miembro No Tutor Dr. VILORIA VERA, DARIO ALFREDO Ph.D.
Tutor Dr. CHACON TORRES, JULIO CESAR Ph.D.

Se presenta el(la) señor(ita) estudiante **QUILUMBA DUTAN, VERONICA ALEXANDRA**, con cédula de identidad No. 1724190358, de la **ESCUELA DE CIENCIAS FÍSICAS Y NANOTECNOLOGÍA**, de la Carrera de **FÍSICA**, aprobada por el Consejo de Educación Superior (CES), mediante Resolución **RPC-SO-39-No.456-2014**, con el objeto de rendir la sustentación de su trabajo de titulación denominado: **Viscosity Analysis of Clay-Carbon Nanotubes Composites as Potential Drilling Muds**, previa a la obtención del título de **FÍSICO/A**.

El citado trabajo de titulación, fue debidamente aprobado por el(los) docente(s):

Tutor Dr. CHACON TORRES, JULIO CESAR Ph.D.

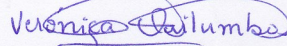
Y recibió las observaciones de los otros miembros del Tribunal Calificador, las mismas que han sido incorporadas por el(la) estudiante.

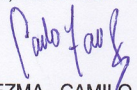
Previamente cumplidos los requisitos legales y reglamentarios, el trabajo de titulación fue sustentado por el(la) estudiante y examinado por los miembros del Tribunal Calificador. Escuchada la sustentación del trabajo de titulación, que integró la exposición de el(la) estudiante sobre el contenido de la misma y las preguntas formuladas por los miembros del Tribunal, se califica la sustentación del trabajo de titulación con las siguientes calificaciones:

Tipo	Docente	Calificación
Presidente Tribunal De Defensa	Dr. ZAMORA LEDEZMA, CAMILO Ph.D.	8,5
Miembro Tribunal De Defensa	Dr. VILORIA VERA, DARIO ALFREDO Ph.D.	10,0
Tutor	Dr. CHACON TORRES, JULIO CESAR Ph.D.	9,8

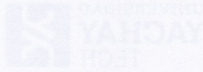
Lo que da un promedio de: **9.4 (Nueve punto Cuatro)**, sobre 10 (diez), equivalente a: **APROBADO**

Para constancia de lo actuado, firman los miembros del Tribunal Calificador, el/la estudiante y el/la secretario ad-hoc.


QUILUMBA DUTAN, VERONICA ALEXANDRA
 Estudiante


 Dr. ZAMORA LEDEZMA, CAMILO Ph.D.
 Presidente Tribunal de Defensa


 Dr. CHACON TORRES, JULIO CESAR Ph.D.
 Tutor



[Signature]

Dr. VILORIA VERA, DARIO ALFREDO Ph.D.
Miembro No Tutor

[Signature]

CIFUENTES TAFUR, EVELYN CAROLINA
Secretario Ad-hoc

Tutor: DR. CHACON TORRES, JULIO CESAR Ph.D.

Miembro No Tutor: DR. VILORIA VERA, DARIO ALFREDO Ph.D.

Presidente Tribunal de Defensa: DR. ZAMORA LEDEZMA, CAMILO Ph.D.

En la ciudad de San Miguel de Urcuquí, Provincia de Imbabura, a los 27 días del mes de agosto de 2019, en el Aula 304, Colectivo de la Universidad de Investigación de Tecnología Experimental Yachay y ante el Tribunal Calificador, integrado por los docentes:

El objeto de la presente es la evaluación de los trabajos de los estudiantes de la carrera de Física, en el curso de Física II, en el semestre de Agosto de 2019, en el aula 304, Colectivo de la Universidad de Investigación de Tecnología Experimental Yachay.

Y habiendo las observaciones de los otros miembros del Tribunal Calificador, las mismas que han sido respondidas por el(a) estudiante.

Finalmente teniendo en cuenta los requisitos legales y reglamentarios, el Tribunal de Defensa, el Tribunal de Evaluación y el Tribunal de Defensa, han acordado la sustentación de los trabajos de los estudiantes de la carrera de Física, en el semestre de Agosto de 2019, en el aula 304, Colectivo de la Universidad de Investigación de Tecnología Experimental Yachay, a las 10:00 horas de la mañana del día 28 de agosto de 2019, en el aula 304, Colectivo de la Universidad de Investigación de Tecnología Experimental Yachay.

Nombre	Apellido	Identificación	Calificación
DR. CHACON TORRES, JULIO CESAR Ph.D.		10.5	7.5
DR. VILORIA VERA, DARIO ALFREDO Ph.D.		10.5	10.5
DR. ZAMORA LEDEZMA, CAMILO Ph.D.		10.5	8.5

Lo que da un promedio de: 8.5 (ocho punto cinco), equivalente a: APROBADO.

Por consiguiente de lo anterior, firman los miembros del Tribunal Calificador, el(a) estudiante y el(a) secretario ad-hoc:

[Signature]
EVELYN CAROLINA CIFUENTES TAFUR
Secretario Ad-hoc

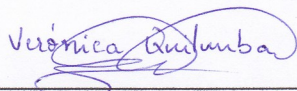
[Signature]
CAMILO ZAMORA LEDEZMA
Presidente Tribunal de Defensa

[Signature]
JULIO CESAR TORRES CHACON
Tutor

AUTORÍA

Yo, **VERÓNICA ALEXANDRA QUILUMBA DUTAN**, con cédula de identidad 1724190358, declaro que las ideas, juicios, valoraciones, interpretaciones, consultas bibliográficas, definiciones y conceptualizaciones expuestas en el presente trabajo; así como, los procedimientos y herramientas utilizadas en la investigación, son de absoluta responsabilidad de el/la autora (a) del trabajo de integración curricular. Así mismo, me acojo a los reglamentos internos de la Universidad de Investigación de Tecnología Experimental Yachay.

Urcuquí, agosto 2019.



Verónica Alexandra Quilumba Dutan
CI: 1724190358

AUTORIZACIÓN DE PUBLICACIÓN

Yo, **VERÓNICA ALEXANDRA QUILUMBA DUTAN**, con cédula de identidad 1724190358, cedo a la Universidad de Tecnología Experimental Yachay, los derechos de publicación de la presente obra, sin que deba haber un reconocimiento económico por este concepto. Declaro además que el texto del presente trabajo de titulación no podrá ser cedido a ninguna empresa editorial para su publicación u otros fines, sin contar previamente con la autorización escrita de la Universidad.

Asimismo, autorizo a la Universidad que realice la digitalización y publicación de este trabajo de integración curricular en el repositorio virtual, de conformidad a lo dispuesto en el Art. 144 de la Ley Orgánica de Educación Superior

Urcuquí, agosto 2019.



Verónica Alexandra Quilumba Dutan
CI: 1724190358

Agradecimiento

La autora de este proyecto, Verónica Alexandra Quilumba Dutan, extiende los más sinceros agradecimientos al Dr. Julio Chacón Torres, quien como tutor de proyecto de titulación, hizo posible el desarrollo de este trabajo. De manera especial, aprecio el tiempo ofrecido para que este proyecto sea llevado de la mejor manera. Además, expreso mi gratitud al Dr. Nicolás Páez y al Dr. Camilo Zamora Ledezma por brindarme la orientación, tiempo y valioso conocimiento para ser capaz de alcanzar el entendimiento necesario para desarrollar esta investigación. En adición, es importante mencionar que este proyecto no habría sido posible sin las herramientas necesarias para su desarrollo experimental, por tal motivo agradezco a MPhil. Christian Narváez y al M.Sc. Luis Carrión, de la Universidad de las Fuerzas Armadas ESPE, por permitirme visitar el Laboratorio de Reología y Fluidos Complejos y utilizar el equipo necesario para la ejecución de este proyecto y por hacer posible la creación de una alianza colaborativa con Yachay Tech. Sin duda, este proyecto no habría sido posible sin la contribución de cada uno de ustedes.

Concluyo expresando mis más sinceros agradecimientos a mi hermano Jorge Luis Quilumba y a mi madre Gricelda Dutan, quienes han sido el gran soporte durante de mi educación universitaria. Sin su ayuda incondicional, la base fundamental de este trabajo no existiría, el conocimiento. Les dedico los resultados de mi trabajo. Además, agradezco a mi padre Jorge, y mis hermanas y hermanos Diana, Johanna, Carlos, y Vinicio quienes han sido mi fortaleza para cumplir mis metas. Cada uno de ustedes me ha enseñado grandes aprendizajes.

¡Infinitas gracias a todos y todas!

Verónica Alexandra Quilumba Dutan

Resumen

Los fluidos de perforación son componentes vitales para facilitar el proceso de perforación en pozos de petróleo y gas. Los pozos de alta temperatura pueden causar dificultades en las operaciones de perforación. Propiedades importantes como la viscosidad del fluido de perforación pueden verse afectadas por el gradiente térmico dentro del pozo. Por ejemplo, un exceso de viscosidad haría que el fluido sea menos bombeable, mientras que si el fluido está muy diluido, disminuirá la capacidad de arrastre de residuos desde el fondo del pozo a la superficie. El papel de un fluido de perforación óptimo es proporcionar lubricación y enfriamiento a través de su conductividad térmica, de modo que el proceso de perforación se lleve a cabo sin complicaciones. La adición de nanopartículas ha demostrado ser una técnica potencial para la mejora de las propiedades reológicas de los fluidos de perforación, debido a sus propiedades intrínsecas fisicoquímicas, eléctricas, térmicas e hidrodinámicas. En este estudio, se realizó un análisis sistemático de viscosidad a partir de nanocompuestos de arcilla bentonita formulados usando nanotubos de carbono de pared múltiple funcionalizados con ácido carboxílico (MWCNT-COOH). Se prepararon varias muestras de nanocompuestos de arcilla combinando arcilla bentonita y diferentes concentraciones de MWCNT-COOH dispersas en agua. Los resultados revelan que la estabilidad de la viscosidad de los nanocompuestos de arcilla en concentraciones de 0.01 % y 0.05 % en peso mejora en condiciones de alta temperatura (50 °C). Finalmente, los resultados presentados en este proyecto de investigación servirán para contribuir al conocimiento en la ingeniería de fluidos de perforación para la industria petrolera ecuatoriana.

Palabras Clave:

Bentonita, Nanotubos de Carbono Multicapa, Fluidos de Perforación Nanoestructurados, Reología, Temperatura.

Abstract

Drilling fluids are vital components to facilitate the drilling process in oil and gas wells.¹ High temperature wells may cause difficulty in drilling operations.² Important properties such as the viscosity of the drilling fluid may be affected by the thermal gradient inside the well. An excess of viscosity would make the fluid less pumpable, whereas if the fluid is very diluted, it will decrease the dragging capacity of the detritus.³ The role of an optimal drilling fluid is to provide lubrication and cooling through its heat capacity and thermal conductivity, so that the drilling process is carried out without complications.⁴ The addition of nanoparticles has proven to be a potential technique in the improvement of the rheological properties of drilling fluids due to their physico-chemical, electrical, thermal, and hydrodynamic intrinsic properties.⁵ In this study, a systematic viscosity analysis from clay-nanocomposites composed of multi-walled carbon nanotubes functionalized with carboxylic acid (MWCNT-COOH) in a matrix of bentonite was conducted. Several samples of clay-nanocomposites were prepared combining bentonite clay and different concentrations of MWCNT-COOH dispersed in water. The results reveal that the stability of viscosity of the clay-nanocomposites in concentrations of 0.01 wt% and 0.05 wt% improves under high temperature conditions (50 °C). In addition, the results presented in this research project will serve to contribute to the knowledge in drilling fluids engineering for the Ecuadorian oil industry.

Keywords: clay, multi-walled carbon nanotubes, nano-based drilling fluid, rheology, temperature, stability, bentonite.

Acknowledgements

The author of this project, Verónica Alexandra Quilumba Dutan, extends the most sincere thanks to Dr. Julio Chacón Torres, who as the thesis tutor made possible the development of this work. In a special way, I appreciate the time given so that this project is carried out in the best way. Also, I express my gratitude to Dr. Nicolás Páez and Dr. Camilo Zamora Ledezma for giving me their help, time and valuable knowledge to be able to reach the necessary understanding to develop this investigation. In addition, it is important to mention that this project would not have been possible without the necessary tools and equipment for experimental development. I would like to thank MPhil. Christian Narváez and M.Sc. Luis Carrión, from the Universidad de las Fuerzas Armadas ESPE, for allowing me to visit the Laboratorio de Reología y Fluidos Complejos and to use equipment necessary for the execution of this project and for making possible the creation of collaborative alliance with Yachay Tech. Without a doubt, this project would not have been possible without the valuable contribution of each one of you.

I conclude expressing my most sincere thanks to my brother Jorge Luis Quilumba and my mother Gricelda Dutan, who have been my greatest support throughout my university education. Without their unconditional support, the fundamental base that makes this work possible would not exist, knowledge. I dedicate to them the results of my work. Also, I thank my father Jorge, and my sisters and brothers Diana, Johanna, Carlos, and Vinicio who have been my greatest strength to accomplish my goals. Each one of you has taught invaluable knowledge.

Infinite thanks to everyone!

Contents

List of Figures	ix
List of Tables	xii
1 Introduction	1
1.1 Structure of Work	2
2 Theoretical Framework	3
2.1 What is a drilling fluid?	3
2.1.1 Components of Drilling Fluids	3
2.1.2 Functions of Drilling Fluids	5
2.1.3 Types of Drilling Fluids	6
2.1.4 Control Parameters for Drilling Fluids	7
2.2 Electronic Properties of Carbon	8
2.2.1 Carbon Nanotubes	10
2.2.2 Single-Walled Carbon Nanotubes	12
2.2.3 Multi-Walled Carbon Nanotubes	12
2.3 Functionalized Carbon Nanotubes	13
2.4 Nano-Based Drilling Fluids (NBDF)	14
2.5 Motivation	15
2.6 General and Specific Objectives	16
2.6.1 General Objective	16
2.6.2 Specific Objectives	16

2.7	Limitations and Scope	16
3	Analysis and Characterization Methods	19
3.1	Ultrasonication and Dispersion Analysis	19
3.1.1	Absorption Spectroscopy	20
3.1.2	Transmittance and Absorbance Measurements	23
3.2	pH Analysis	24
3.2.1	Experimental Determination of pH	25
3.3	Rheology: Basic Concepts	26
3.3.1	Parameters Affecting Viscosity	27
3.3.2	Rheological Analysis	27
4	Methodology	31
4.1	Formulation of MWCNT-COOH Dispersions for Absorption Tests	31
4.1.1	Material Selection	31
4.1.2	Sample Preparation	31
4.1.3	Absorption Measurements	32
4.2	Formulation of the Nano-Based Drilling Fluid	33
4.2.1	Material Selection	33
4.2.2	Sample Preparation	33
4.2.3	Rheological Measurements	35
5	Results & Discussion	39
5.1	Absorption Analysis of MWCNT-COOH Dispersions	39
5.2	Rheological Analysis of the Nano-Based Drilling Fluid	41
5.2.1	pH Analysis	41
5.2.2	Viscosity Analysis	42
5.2.3	Viscosity vs. Concentration of MWCNT-COOH	47
5.2.4	Viscosity vs. Temperature	51
6	Conclusions & Outlook	59
7	Appendix	61

List of Figures

2.1	Atomic Structure of Bentonite Clay	4
2.2	Functions of Drilling Fluids	6
2.3	Electron Configuration of Carbon	9
2.4	Types of molecular bonds formed by valence electrons of carbon	9
2.5	Representation of a Graphene Sheet	10
2.6	Single- and Multi-Walled Carbon Nanotubes	12
2.7	Limitations and Scope of the Project	17
3.1	Electronic Transition of Electrons	20
3.2	Transmittance Phenomenon of Liquid Samples	21
3.3	Transmittance and Absorbance Measurements	23
3.4	Experimental Determination of pH	25
3.5	Rheological Behavior of Matter	26
3.6	DHR Rheometer	28
3.7	DHR Rheometer: Peltier Concentric Cylinder System	29
3.8	DHR Rheometer: DIN Rotor	29
4.1	MWCNT-COOH Dispersions	32
4.2	Nano-based drilling fluids	33
4.3	Structural Constructive Measurements	37
4.4	Structural Destructive Measurements	38
5.1	Absorption Analysis of MWCNT-COOH Dispersions	41

5.2	Structural Constructive and Destructive Analysis of samples AP-2 and EE-2 at 25°C	44
5.3	Structural Constructive and Destructive Analysis of samples BP-2 and FE-2 at 25°C	45
5.4	Structural Constructive and Destructive Analysis of samples CP-2 and GE-2 at 25°C	46
5.5	Structural Constructive and Destructive Analysis of the Nano-Based Drilling Fluid with Peruvian Bentonite at 25°C	49
5.6	Structural Constructive and Destructive Analysis of the Nano-Based Drilling Fluid with Ecuadorian Bentonite at 25°C	50
5.7	Structural Constructive and Destructive Analysis of composites formulated with Peruvian and Ecuadorian Bentonite, and 0.00 wt% of MWCNT-COOH at 50°C	53
5.8	Structural Constructive and Destructive Analysis of composites formulated with Peruvian and Ecuadorian Bentonite, and 0.01 wt% of MWCNT-COOH at 50°C	54
5.9	Structural Constructive and Destructive Analysis of composites formulated with Peruvian and Ecuadorian Bentonite, and 0.05 wt% of MWCNT-COOH at 50°C	55

List of Tables

4.1	MWCNT-COOH Dispersions for Dispersion Tests	32
4.2	Synthesis of MWCNT-COOH Dispersion to Formulate the NBDFs	34
4.3	Nano-Based Drilling Fluid Formulation	35
5.1	pH Measurements of the Nano-Based Drilling Fluid	42
5.2	Viscosity Results at 25°C	48
5.3	Viscosity Results at 50°C	52
7.1	Allotropic forms of element carbon	62

Chapter 1

Introduction

The present study brings together the results found during the research work entitled "*Viscosity Analysis of Clay-Carbon Nanotubes Composites as Potential Drilling Muds*". This analysis is based on a study on the influence of multi-walled carbon nanotubes functionalized with carboxylic acid (MWCNT-COOH) on the rheological properties of a simple drilling fluid when it is subjected to high temperatures.

The investigation was carried out due to the importance of drilling fluids, since they are a vital component during the extraction process in gas and oil wells.¹ Several studies indicate that high temperatures in drilling wells can cause difficulties in the extraction process because the properties of the drilling fluid can be affected by the geothermal gradient inside the well.^{2,3}

To carry out the study, a total of six samples were formulated using natural sodium bentonite, different concentrations of MWCNT-COOH (0.01 wt% and 0.05 wt%), and distilled water. Three of the six samples were prepared using Ecuadorian natural sodium bentonite and the other three were prepared using Peruvian natural sodium bentonite. Then, all the samples were subjected to a rheological characterization for the analysis of the viscosity at different temperatures (25°C and 50°C).

The objective of this work is to generate unprecedented knowledge around the use of nanostructured bentonite clay with multi-walled carbon nanotubes as a potential drilling fluid. The results obtained from the rheological analyses will prove the possibilities of using this nano-based drilling fluids in the Ecuadorian drilling oil industry.

1.1 Structure of Work

All the contents of this document are oriented to guide the reader to a good understanding of the results reported in this research. In this first introductory chapter, the topic, the importance, the method, and the objective of this work are presented. Chapter two starts with a theoretical framework which introduce basic concepts of drilling fluids, such as the components, functions, types and control parameters of drilling fluids. In the subsequent, a brief explanation of carbon nanotubes, their functionalization, and the concept of nano-based drilling fluids is presented. In Chapter three, the characterization methods used in this research project are explained, followed by the methodology carried out during the experimental part in chapter four. The methodology also contains the formulation of all the samples used in this investigation. Finally, the results and discussions about the data obtained during measurements are shown and discussed in chapter five. This work ends in chapter six with conclusions and outlook.

Chapter 2

Theoretical Framework

2.1 What is a drilling fluid?

Pål Skalle, in his book *Drilling Fluid Engineering*, states that the simplest drilling fluid results from a mixture of water and clay. Skalle also mention that drilling fluids are often referred to as drilling muds which circulates to bring cuttings from the bottom of the wellbore to the surface.⁶ Drilling fluids have converted into vital components to enhance and optimize the production of oil and gas.¹ They are used to guarantee efficient drilling and to control the pressure of the wellbore and to stabilize it.⁷ Drilling fluids show non-Newtonian, elastic and thixotropic behaviors.⁸ In addition, drilling fluids have a continuous phase, which is liquid, and a discontinuous phase which is composed by solids.⁹

2.1.1 Components of Drilling Fluids

As mentioned earlier, the simplest drilling fluid is a mixture of water and clay. However, environments where fluids are used have varying conditions of temperature and electrolytes which causes variations in flow properties, therefore, additives are usually added to the simple fluid in order to control its physical properties.¹⁰ In this section one of the main components of the drilling fluids is introduced, clays. In addition, the most common additives used during the formulation of a drilling fluid are briefly detailed.

- **Clays**

Clay minerals are key components in the formulation of drilling fluids since they provide acceptable particle

dispersion. This factor is vital to obtain a stable composite.¹⁰ As can be seen in figure 2.1, clays are composed of layers comprising silica and alumina sheets forming a stacked structure.¹⁰ According to Luckham and Rossi, in their article *"The Colloidal and Rheological Properties of Bentonite Suspensions"*, the most clay minerals are composed by two structural units forming their atomic lattices. The first unit is an octahedral structure which consist of two sheets of oxygens and hydroxyls which fix aluminum, iron, or magnesium atoms in octahedral coordination. The second unit is the tetrahedral sheet composed by silica tetrahedrons distributed to form an hexagonal system repeated until forming a sheet with stoichiometry $Si_4O_6(OH)_4$, (see Figure 2.1).¹⁰

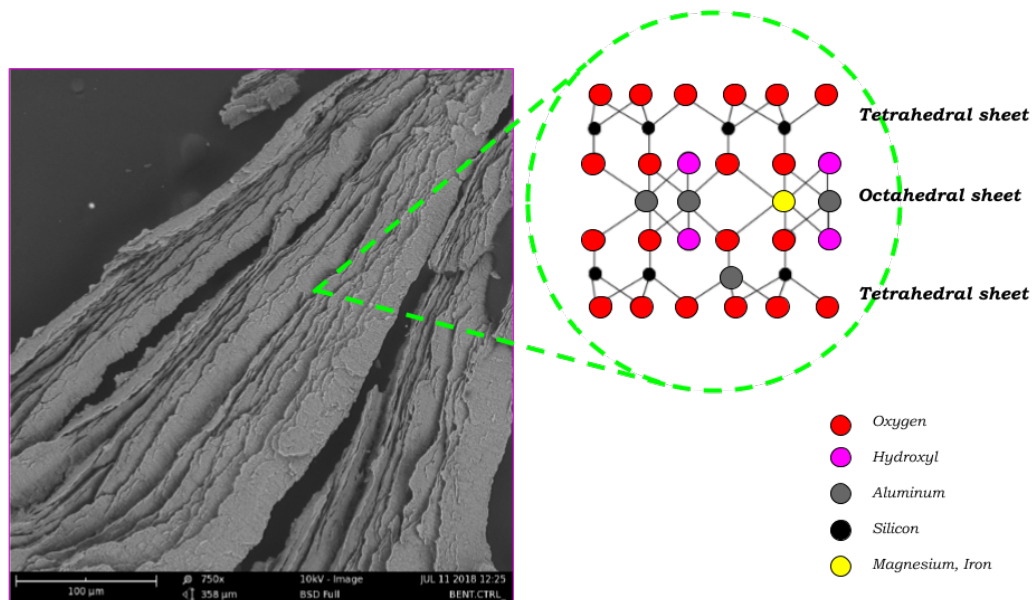


Figure 2.1: Representation of the atomic structure of montmorillonite mineral, the main component of bentonite clay. Image adapted. Original Image: Reference [10]

Figure 2.1 is a representation of the atomic structure of montmorillonite. In the atomic structure, shared oxygen atoms between sheets and the surface of the layers with high repulsive potential resulting from isomorphous

substitution, provide an increment of the basal space between layers when water is penetrating.¹⁰

When Na^+ cations are exchanged with the surface of the montmorillonite, sodium montmorillonite is formed. The stoichiometry of sodium montmorillonite is $(Na_{0.33} [(Al_{1.67}Mg_{0.33})(O(OH))_2(SiO_2)_4])$ and it is also known as sodium bentonite.¹⁰ Sodium bentonites have high swelling capacity and other remarkable rheological properties, for this reason they are preferred in the formulation of drilling fluids for the oil industry.¹¹

- **Additives**

According to B. Abu-Jdayil and Ghannam, one of the most important factors during the formulation of drilling fluids is the chemical additive. The mentioned authors indicate that additives such as electrolytes, polymers, and surface active agents, combine with bentonite particles and change the rheological properties of the fluid.¹¹ Some examples of polymers used in the conformation of bentonite suspensions are: poly vinyl pyrrolidone, poly vinyl alcohol, xanthan, polyanionic cellulose, polyethyleneimine, and ethylene glycol. These polymers reduce filtration, flocculation, and enhance the drag capacity of the fluid. In addition, the mentioned study indicate that carboxymethyl cellulose helps to control viscosity and fluid losses. Also, it helps to maintain the rheological properties of the drilling fluid at high temperatures, pressures, and salinities.¹¹ Another study conducted by Ismail AR. mentions that the addition of potassium chloride (KCl) helps to control the rheological properties of drilling fluids and provide better hydration-resistance.¹² On the other hand, a research carried out by Amanullah et al., indicates that the addition of nanomaterials has proven to be a potential technique in the improvement of the rheological properties of drilling fluids due to their physico-chemical, electrical, thermal, and hydrodynamic characteristics.⁵

2.1.2 Functions of Drilling Fluids

As mentioned in section 2.1, drilling fluids are vital components during oil extraction. For this reason, they require the evaluation of key parameters to control their physical properties and ensure that the fluid fulfills its functions optimally.

As illustrated in the figure 2.2, once the fluid has been pumped through the drill string, it must be able to remove the cuttings from the bottom of the hole to the surface and clean the well.⁴ If the circulation process stops, the fluid must keep the detritus in suspension. It must cool, lubricate and control the corrosion of the drill during the drilling process. Additionally, it is necessary that the fluid maintain the stability of the well controlling the pressures of the subsoil.³

Each mentioned function modulates the correct extraction process. For example, if the temperature and pressure

of the well increases, the fluid must be able to maintain its properties to avoid difficulties in the operation. In the following chapter, the control parameters will be fully covered.

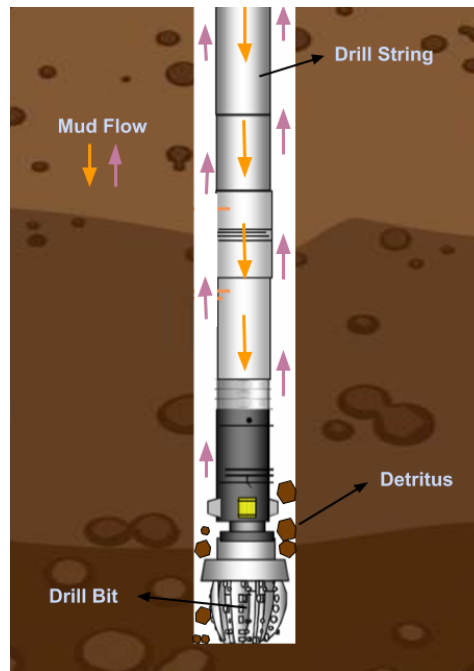


Figure 2.2: Process of circulation of the drilling fluid through the well.

2.1.3 Types of Drilling Fluids

There are three main types of drilling fluids used to drill oil and gas wells: oil-, synthetic-, and water-based drilling fluids.¹²

- **Water-Based Drilling Fluids (WBDF)**

WBDF have water as their continuous phase.⁷ WBDF are complemented with additives such as activity salts, viscosifiers, filtrate reducers, and hydrate resistant polymers.¹² WBDF are mostly used because they considered inexpensive and environmentally friendly.¹²

- **Oil Based Drilling Fluids (OBDF)**

This class of drilling fluid contains oil as its continuous phase.⁷ OBDF are called "*oil base mud*" if they contain 1-15% water, and "*inverse emulsion*" if they contain 15-50 % water. In OBDF, solids are considered inert

because they do not react with oil.⁴ Additionally, OBDF avoid corrosion to the auger and the string, avoid sensitive clay problems, increase the perforation rate, and avoid formation damage. In contrast with WBDF, OBDF have high initial and maintenance costs as well as a high level of pollution towards the environment.⁴

- **Synthetic Based Drilling Fluids (SBDF)**

SBDF contain a synthetic organic compound as their continuous phase and other ingredients such as emulsifiers, barite, clays, lignite, and lime as additives.¹³ They are also composed of olefins, esters, and paraffins.⁷ When a salt brine is dispersed in the synthetic organic compound, it forms an emulsion. SBDF are used for deep water drilling processes. They have a low bio-availability and toxicity.¹³ These synthetic-base systems are environmentally-safer alternatives to traditional oil-base systems.¹⁴ Additionally, oil and synthetic based fluids provide natural lubrication and are considered non-corrosive.¹⁴

2.1.4 Control Parameters for Drilling Fluids

Espinoza, C. defines viscosity, thixotropy, pH, density, sand content, and mud-cake thickness as primordial characteristics of a drilling fluid.³ These control parameters are described below.

- **Viscosity**

Viscosity is the property that represents the internal resistance of a fluid to motion.¹⁵ In the particular case of drilling fluids, an optimal level of viscosity is required. If there is an excess of viscosity, the fluid is less pumpable because the drag capacity will increase. On the other hand, if the fluid is very diluted, the drag capacity will decrease and the concentration of cutting at the bottom of the well will stuck the drill.³

- **Thixotropy**

Thixotropy is a non-Newtonian property, which depends on time.³ It is described as the decrease in apparent viscosity due to the structural destruction of the suspension caused by shear stresses, followed by a structural construction in time when there is no more effort.³

- **pH**

During the formulation of drilling fluids, a basic pH is required.³ It is important to maintain a basic range since organic dispersands and filtration control additives are more effective in alkaline environments, corrosion and contaminating electrolytes are averted, and bacterial action is retarded.¹⁴ A variation on pH due to the presence of salts in the drilling well can cause the sedimentation of the particles and the perforation of the material.³

- **Density**

The density allows the mud to exert back pressure on the walls of the drilling well by controlling the lithostatic and hydrostatic pressure of the formations.³ It influences the carrying capacity of the cuts.³

- **Solids Content**

Rheological properties of the drilling fluid are controlled by the quantity, size, and type of suspended solids. The total of solids in a drilling fluid is composed of different concentrations of bentonite, sand, weighting materials, and additives.¹⁴ The content of solid increases as the drilling process takes place. As a result, its rheological conditions change causing the wear of the pumps.³

- **Mud-cake Thickness**

Mud-cake is formed when colloidal particles create a waterproof layer that provides cohesion to the walls of the perforated well, preventing its collapse and waterproofing it.³ During the formulation of a drilling fluid it is necessary to avoid the mixture of components that promote the creation of large pores, like coarse particles. Bentonite clays characterize to form a mud-cake with low permeability due to their small irregular shape platelets which compact under pressure avoiding filtration.¹⁴

In recent years, several investigations about the rheological properties of drilling fluids have been carried out. Studies indicate that including additives to the fluid, control parameters are enhanced.¹² Ismail A.R., in his article "*The application of MWCNT to enhance the rheological behavior of drilling fluids at high temperature*", mentions that a little addition of nanoparticles, specifically multi-walled carbon nanotubes (MWCNT) which will be introduced in the following section, increases the viscosity when temperature rises.¹ As mentioned in the introduction, the purpose of this research is to study the behavior of viscosity when carbon nanotubes are added as additive to the drilling fluid. Therefore, in order to guide the reader towards a good understanding of the present work, carbon, its electronic structure, and its allotropes are introduced in detail.

2.2 Electronic Properties of Carbon

According to Falcao and Wudl, carbon compounds exceed 95% of all chemical compounds. They also mention that carbon can form compounds with electronegative and electropositive elements and that it can form compounds with itself through single, double, and triple bonds.¹⁶

The atomic number of carbon is six. Then, its electronic configuration is a representation of an arrangement of those six electrons.¹⁷ Figure 2.3 shows the arrangement of carbon electrons, which consists in the distribution of two

electrons in orbital s of the first energy level $n=1$ and 4 electrons in the orbitals s and p of the second energy level $n=2$. Thus, the electronic configuration of carbon is $1s^2, 2s^2, 2p^2$.¹⁷

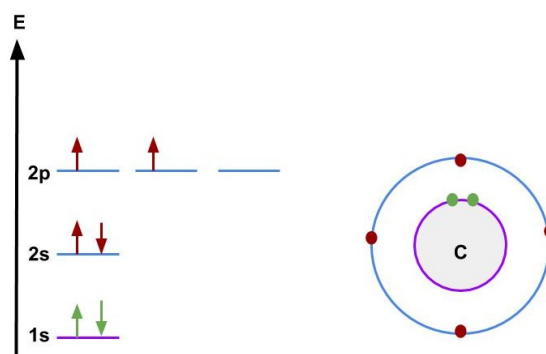


Figure 2.3: Representation of the electronic configuration of carbon. The figure shows the arrangement of the six carbon electrons. As it can be seen, two electrons are located in the orbital s of the first energy level $n=1$ and 4 electrons in the orbitals s and p of the second energy level $n=2$.

Electrons located at level $n=1$, in the $1s$ orbital, do not participate in the hybridization phenomena because they constitute the *core* of the atom. However, electrons located in the orbitals $2s$ and $2p$ participate in the hybridization phenomena and they are called valence electrons. Valence electrons can form four types of bonds that are illustrated in figure 2.4; 4 simple bonds, 1 double and 2 simple bonds, 2 double bonds, and 1 triple and 1 simple bonds.¹⁷ When the orbitals of the $2s$ level combine with the $2p$ orbitals new orbitals called "*degenerated orbitals*" are generated.¹⁷ Thus, the capacity of hybridization of atomic carbon orbitals generates carbons of sp^3 -, sp^2 -, sp -nature, which confers carbon a unique situation for the construction of a variety of structural modifications or allotropic forms such as diamond (sp^3), fullerene (sp^2), graphene (sp^2), graphite (sp^2), and carbon nanotubes (sp^2).¹⁸

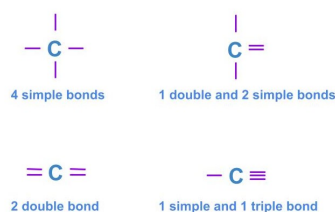


Figure 2.4: Types of molecular bonds formed by valence electrons of carbon

As it was mentioned at the beginning of this work, the purpose of this research is to analyze the effect of carbon nanotubes on the viscosity of a simple drilling fluid. Therefore, the following subsection will explain the importance of carbon nanotubes in this research. In addition, the rest of the mentioned allotropic forms of carbon and its main properties are presented in Appendix section.

2.2.1 Carbon Nanotubes

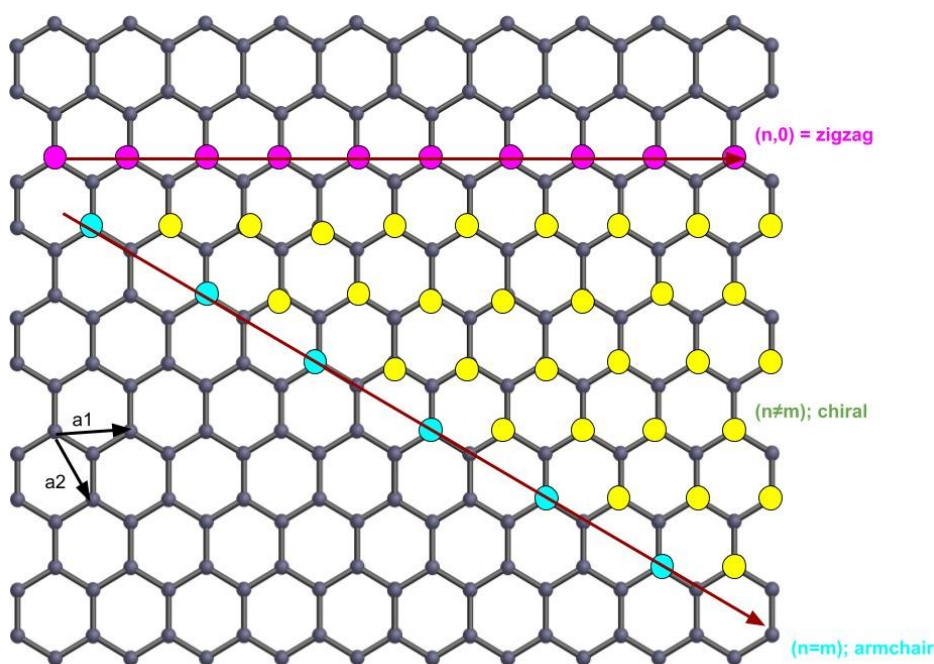


Figure 2.5: Representation of a graphene sheet. The graphene sheet is defined by the indices n, m . If $m=0$ (violet circles), the nanotubes are called *zigzag* nanotubes, if $n=m$ (sky blue circles), the nanotubes are called *armchair* nanotubes, otherwise, they are called *chiral* (yellow circles).

The discovery of carbon nanotubes (CNTs) is attributed to Sumio Iijima when, in 1991, he detected microtubules of graphitic carbon with outer diameter of 4-30 nm and a length of up to $1 \mu\text{m}$.¹⁹ According to Iijima, the discovered microtubules were constituted by multiple graphene cylinders concentrically arranged whom he called multi-walled carbon nanotubes.¹⁹

According to Ariza A. and Casas J., CNTs are cylinders originated from the winding on itself of a sheet of

graphene, joining its edges. They also mention that the ends of CNTs can be open or closed with a hemisphere.²⁰ CNTs are defined by a network of sp^2 hybridized carbon atoms.²¹ As seen in figure 2.5, the way the graphene sheet is rolled up is represented by their chirality and so-called (n, m) -indices which denote the number of unit vectors along two directions in the crystal lattice of the graphene sheet.^{21, 22} Three types of CNTs can be observed depending on the directionality of the graphene sheet. For instance, if $m=0$, the nanotubes are called *zigzag* nanotubes, if $n=m$, the nanotubes are called *armchair* nanotubes, and if $n \neq m$ the nanotubes are called *chiral*.²²

Carbon nanotubes possess notable electronic properties. They exhibit either metallic or semiconducting behavior depending on the (n, m) -indices.²¹ In addition, CNTs have superior electrical, chemical, and mechanical properties which makes them ideal candidates for novel structures such as nanocomposites.²³ Their unique stiffness, bending, strength, and high aspect ratio properties can be used to reinforce polymers and other materials.²¹ For instance, the tensile strength of CNTs is up to 20 times higher than that of the best steels. Their rigidity is characterized by a Young's modulus five times greater than steel. Additionally, CNTs are electrical and thermal conductors.²⁰ Jorio et al., in their book "*Carbon nanotubes: advanced topics in the synthesis, structure, properties and applications*", mention that the Young modulus of carbon nanotubes exceeds 1 TPa. The authors also mention that this is a beneficial property to fortify composites based on carbon nanotubes.²⁴ All the mentioned properties depend on the diameter, length and chirality of CNTs.²⁰

Another beneficial property of CNTs is their thermal conductivity.²⁵ According to Jorio et al., the network of sp^2 hybridized carbon atoms that constitute CNTs provides them of enough strength to maintain a superior thermal conductivity compared to other materials, like diamond. This property let them to remain stable at very high temperatures (near to 4000 K, the melting point of graphite). Jorio et al. also mention that CNTs have better structural stability than graphene due to their cylindrical shape.²⁴ All the mentioned properties provide CNTs the advantage of having remarkable applications for novel structures such as nanocomposites, nano-probes, nano-actuators, nano-vessels for hydrogen storage and gene delivery systems, and nano-scale electronic devices in nano-electromechanical systems.²³

On the other hand, one of the challenges in the search for enhancing the properties of CNTs lies in their low dispersion in usual organic solvents.²⁰ Jorio et al. also mention that obtaining a uniform dispersion and alignment of CNTs in a matrix is a problem that reduce the performance of their potential properties.²⁴ However, this problem can be solved by using polar solvents or by adding functional groups to the surface of CNTs.²⁰

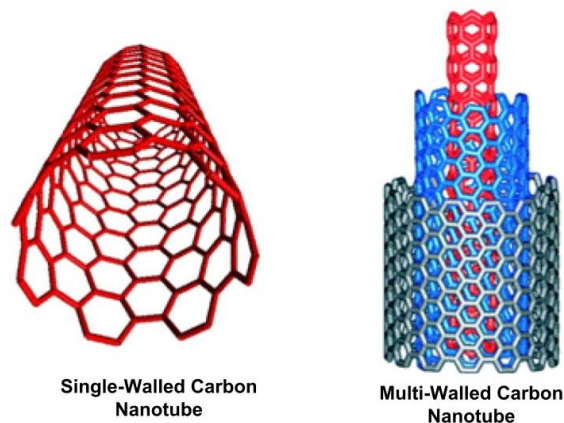


Figure 2.6: Single- and Multi-Walled Carbon Nanotubes. Image adapted. Original Image: Reference [26]²⁶

2.2.2 Single-Walled Carbon Nanotubes

Single-walled carbon nanotubes (SWCNTs) were discovered in 1993.²⁰ Iijima S. mentions that SWCNTs are cylinder made of a single graphene sheet rolled up to form a tube as seen in figure 2.6, their diameter ranges from 0.4 to 2-3 nm, and their length reach the micrometer scale.¹⁹ Similar to CNTs, SWCNTs can be either metallic or semiconducting depending on the chiral vector. For instance, if the difference of the vector integer $n-m$ is a multiple of three, the nanotube is metallic. Otherwise, it is semiconducting.²⁷ Between the outstanding properties of SWCNTs, highlights their mechanical strength greater that that of Fe, their density lower than that of Al, and their thermal stability at 1400 °C in vacuum.¹⁹

2.2.3 Multi-Walled Carbon Nanotubes

As mentioned in section 2.2.1, Sumio Iijima discovered multiwalled carbon nanotubes (MWCNT) in 1991. He described MWCNTs as microtubules of graphitic carbon with outer diameter of 4-30 nm and a length of up to 1 μm .¹⁹ According to Harris P., the synthesized microtubules by Iijima contained at least two graphitic layers with inner diameters of around 4 nm. Harris also mention that, in general, the length of MWCNTs ranges from tens of nanometers to several micrometers and that their outer diameter ranges from about 2.5 nm to 30 nm.²⁸ Since the discovery of Iijima, MWCNTs were defined as concentric multiple rolled layers of graphene, as can be seen in figure 2.6.²⁰ The separation between each of the MWCNT sheets is approximately 0.34 nm.²⁰ In addition, MWCNTs

exhibit advantages over CNTs and SWCNTs such as ease of mass production, low cost product per unit, and enhanced thermal and chemical stability.²⁹

Due to the great variety of properties that carbon nanotubes and multi-walled carbon nanotubes possess, several studies have been carried out in order to take advantage of them. As mentioned before, one of the challenges in the search for enhancing the properties of CNTs lies in their low dispersion in usual organic solvents.²⁰ Functionalization is one of the techniques used to enhance the mechanical and electrical properties of carbon nanotubes. Additionally, functionalization contributes to water-solubilization of carbon nanotubes.²⁹ In the following section, this technique is explained.

2.3 Functionalized Carbon Nanotubes

Currently, carbon nanotubes are used for a wide variety of applications including their incorporation in composite materials as structural reinforcement.²⁰ The maximization in the use of their mechanical, thermal, electrical, and chemical properties is limited by their low solubility and the lack of uniform dispersion and alignment in a matrix.^{21, 24} For example, a great part of forms of carbon nanotube material are insoluble in organic solvents, making it difficult to explore and understand their chemistry at the molecular level.³⁰ The problem of separation and dispersion of CNTs can be solved by functionalization.²¹

Surface modification of CNTs is performed for applications that require organic solvents or water-solubilization.²⁹ The most recognized technique to maximize the mechanical properties of composites structured with CNTs is the chemical functionalization.³¹ An study performed by Jian Chen et al., reports that the application of heat for a long time to SWCNT-COCl functionalized with a long-chain molecule octadecylamine ($C_{18}H_{39}N$) cause their volume expansion, due to the exfoliation of the nanotubes bundles, producing individual nanotubes and collaborating with their optimal dispersion in chloroform, dichloromethane, aromatic solvents, and CS_2 .³⁰

On the other hand, Vikas Mittal in his book "*Polymer nanocomposite coating*" mentions that joining carboxyl groups (-COOH) or hydroxyl groups (-OH) on the surface of CNTs is a typical step of functionalization to provide homogeneous dispersion of CNTs in the composite matrix. He also mention that the dispersibility in water and organic solvents of nanotubes functionalized with carboxylic groups (CNT-COOH) is better than pristine CNTs.³¹ In the particular case of MWCNTs, an study conducted by Choi and Zhang reports that MWCNT-COOH are obtained via oxidation using acids such as ozone or plasma, which creates oxygen functional groups (e.g., -OH, -C=O), so that the presence of oxygen-containing groups promotes the exfoliation of CNT bundles. Choi and Zhang emphasize that MWCNTs functionalized with COOH (carboxylic acid) enhance their solubility in polar media.²⁹

In this research project, it is required to obtain an optimal dispersion of carbon nanotubes in aqueous solutions before adding them to the drilling fluid to form the composite. Some studies report excellent results of dispersion of pure carbon nanotubes in aqueous solutions by using surfactants.³¹ However, including more components, such as surfactants, to the drilling fluid is not convenient due to the increasing of cost of production and the environmental impact. For these reasons, functionalized carbon nanotubes are the best option to solve the problem of dispersion of nanotubes in water.

On the other hand, functionalization is a process that could affect some electrical and mechanical properties of carbon nanotubes. For example, the properties of SWCNTs change due to the structural defects occurred by C=C bond breakages during chemical processes. However, intrinsic properties of MWCNTs are preserved.²⁹ This fact should be taken into account during the formulation of the drilling fluid.

2.4 Nano-Based Drilling Fluids (NBDF)

A drilling fluid can be considered a nano-based drilling fluid when it contains at least one additive with a particle size in range of 1-100 nm.⁵ According to Amanullah et al. nanoparticles have more than thousand times higher surface area to volume ratio than microparticles and million times higher surface area to volume ratio than macroparticles. The previous author also emphasizes that the role of the surface area to volume ratio and the Van der Waals, molecular and atomic forces influences the behavior of a fluid system with minimum concentration of nanomaterial (<1%).⁵

Several studies report a wide variety of beneficial properties of fluids based on nanoparticles. For instance, Nadeem et al. report that nanofluids possess enhanced thermal conductivity which reduces the cooling cost of some industrial processes.³² Amanullah et al. mention that the huge surface area to volume ratio of nanoadditives improves the thermal conductivity of nano-based fluids providing efficient cooling of the drill bit and avoiding costs related to equipment damage, repair, failure and replacement.⁵ Kamel et al. mention that nanoparticles offer high heat transfer rate to the fluid system and that the successful employment of nanofluids can result in significant energy and cost savings.³³ Wong K. and Leon O. mention that nanofluids possess enhanced thermophysical properties such as thermal conductivity, thermal diffusivity, viscosity and convective heat transfer coefficients compared to oil and water based drilling fluids.³⁴ In addition, the use of nanoparticles results environmentally friendly due to the extremely low concentration of nanoadditive (<1%) required to formulate a nanofluid.⁵

On the other hand, an experimental study conducted by Ismail et al. reports data about the influence of nanoparticles on the rheological properties of water based drilling fluids. For example, the addition of nanoparticles such as nanosilica, glass beads, and MWCNT to water based drilling fluids reveals an improvement in some control

parameters such as plastic viscosity, lubricity, yield point, gel strength, and mud cake thickness.¹² Choi et al. also mention that the addition of low concentration of nanoparticles change the thermal conductivity and the viscosity of ordinary fluids.²⁹ An study carried out by Timofeeva et al. suggest that the shape of particles also contributes to improve the thermal properties of a fluid.³⁵ According to Elias et al. the cylindrical shaped nanoparticles offered the higher heat transfer rate as compared to the other shaped particles.³⁶

Taking into account all the mentioned information, the challenge of this research project is to analyze the effect of nanoparticles, such as MWCNT-COOH, over the viscosity of a simple drilling fluid formulated with bentonite, carbon nanotubes, and water, aiming for an increase in the viscosity.

2.5 Motivation

In the previous section, it was mentioned some of the effects of nanoparticles over the rheological properties of a fluid system. It was also mentioned that thermal conductivity of nanoparticles make them a unique material for the enhancement of the rheological properties of drilling fluids. A large number of experimental investigations have been conducted in order to improve the rheological behavior of drilling fluids to make them more suitable for modern oil drilling engineering. Nowadays, several studies about formulation of drilling fluids using nanoparticles have been reported, as mentioned in the previous section. Many of these studies have been carried out using nanoparticles and natural sodium bentonite as the discontinuous phase, and water as the continuous phase.¹ In addition, most of these studies use natural sodium bentonite from various mineral deposits such as Germany, Scotland, France, Spain, Holland, among others.³ However, studies carried out about NBDF containing sodium bentonites from South American deposits are scarce. For example, in Ecuador, the most common mineral clay for industrial applications, including the production of drilling fluids is Peruvian sodium bentonite.³ Therefore, in this research project, a NBDF will be formulated using MWCNT-COOH and natural sodium bentonite from Peruvian and Ecuadorian origins. This project will be performed in order to contribute with the knowledge in drilling engineering for the Ecuadorian oil industry. Finally, in order to understand the rheological behavior of the formulated NBDF, rheological measurements will be performed. Additionally, dispersion analyses of MWCNT-COOH will be performed to ensure an homogeneous mixture with bentonite clay.

2.6 General and Specific Objectives

2.6.1 General Objective

The general objective of the project is to analyze the rheological behavior of nanostructured drilling fluid based on water, MWCNT-COOH, and natural sodium bentonite extracted from mineral deposits from Perú and Ecuador.

2.6.2 Specific Objectives

- Achieve the most optimal dispersion of MWCNT-COOH in aqueous solutions to obtain an homogeneous NBDF.
- Perform a pH study of the formulated NBDFs in order to analyze the influence of MWCNT-COOH.
- Analyze the viscosity of the formulated NBDF to study the influence of MWCNT-COOH over the rheological properties of the fluid.
- Determine the most optimal concentration of MWCNT-COOH from the samples prepared with Peruvian and Ecuadorian sodium bentonite based on the results obtained from rheological characterization.

2.7 Limitations and Scope

Figure 2.7 shows the scope and the limitations of the project. First of all, five samples will be synthesized to analyze the dispersion of MWCNT-COOH in distilled water. Then, absorption analysis will be performed to the samples in order to know the most optimal time of ultrasonication to achieve the most optimal dispersion of nanotubes. Once the optimal time is determined, nanostructured composites will be formulated using distilled water, bentonite clay, and different concentration of MWCNT-COOH. Then, rheological measurements will be done to the composites. The analysis will start with the application of step jump tests in order to determine the adequate range of shear rates and the time were viscosity varies considerably. Then, the official measurements will be carried out by applying structural constructive and destructive measurements at two different temperatures, 25°C and 50°C. Finally, the results obtained will be analyzed taking into account the behavior of viscosity at different concentrations of MWCNT-COOH and different temperatures to bring come conclusions around the composite material.

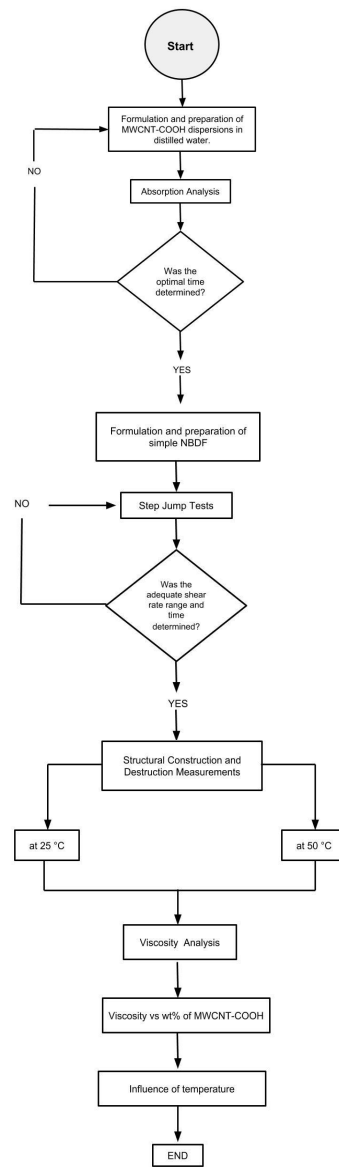


Figure 2.7: Limitations and Scope of the Project

Chapter 3

Analysis and Characterization Methods

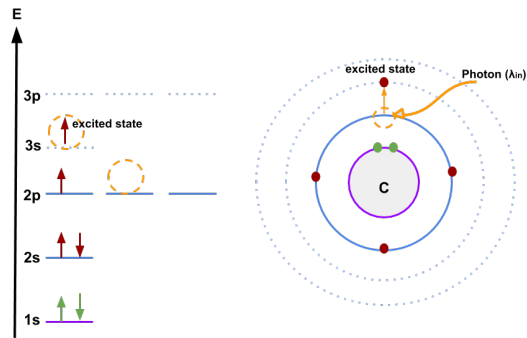
3.1 Ultrasonication and Dispersion Analysis

Due to the adhesion forces between nanoparticles, agglomeration and settlement can be observed.³⁷ The aggregation of nanoparticles and its size can cause sedimentation, decreasing the thermal conductivity and affecting the viscosity of nanofluids.³⁸ According to Mahbulul et al. well dispersed nanoparticles help to maintain the stability of nanofluids, avoiding aggregation and, consequently, sedimentation.³⁷

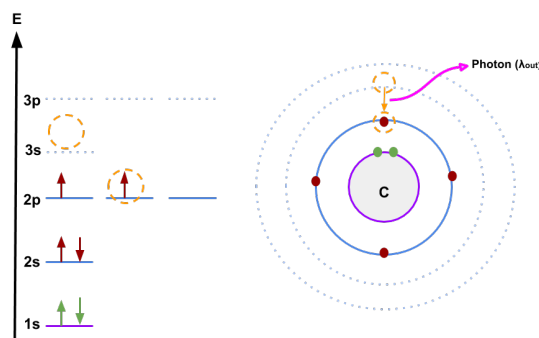
Through a dispersion process, a stable nanofluid free of aggregation and sedimentation can be achieved.³⁷ Dispersion is the process that separates the smallest dispersible particle from an agglomerate and mixed it in the host matrix system.³⁹ In previous sections it was mentioned that it is important to obtain an optimal dispersion of nanoparticles before to formulate a nano-based drilling fluid in order to obtain an homogeneous fluid. A widely used method for dispersion is ultrasonication.³⁹

Studies have reported that ultrasonication methods dissolve agglomeration and improve the dispersion of nanoparticles since they affect their surface and structure.³⁸ In the specific case of carbon nanotubes, dispersion is used to analyze the individualization of carbon nanotubes.³⁹ According to Njuguna et al. the dispersion of CNTs as individuals is important to maximize the translation of CNT properties to the composites.³⁹ Thus, using ultrasonication, uniformly dispersion of CNTs in the host matrix can be achieved.³⁹ During the ultrasonication process, CNTs are premixed in dispersion media by a standard stirrer and then homogenized by ultrasound.³⁹ The effect of ultrasound in CNTs is important because of their high aspect ratio. However, the length of CNTs is reduced due to the force created during sonication time.³⁸

3.1.1 Absorption Spectroscopy



(a) Unstable (excited) state



(b) Stable stable

Figure 3.1: Process of absorption of incident light with wavelength λ_{in} carried by the atom. **(3.1a)** Incident light has enough energy to excite an electron to another electronic state with higher energy. The new excited state in which the electron is located is unstable. **(3.1b)** After being in the unstable state, the electron fall to the state of lower energy by emitting a photon λ_{out} with the same energy as the difference between energy levels.

According to atomic absorption theory, atoms absorb incident light at a definite wavelength. Incident light (λ_{in}) has enough energy to excite electrons to another electronic state. The electron is excited to a higher energy state by absorption of energy as can be seen in figure 3.1a. The new excited state in which the electron is located is unstable, thus the electron will quickly fall to the state of lower energy by emitting a photon with the same energy as the difference between energy levels as seen in figure 3.1b. This process is called electronic transition.⁴⁰

Joseph von Fraunhofer did the first observation of atomic absorption while studying dark lines in the solar spectrum. Then, in 1955, Alan Walsh applied absorption spectroscopy to chemical analysis. Since then, absorption spectroscopy have replaced many difficult and time consuming methods for absorption analysis.⁴⁰

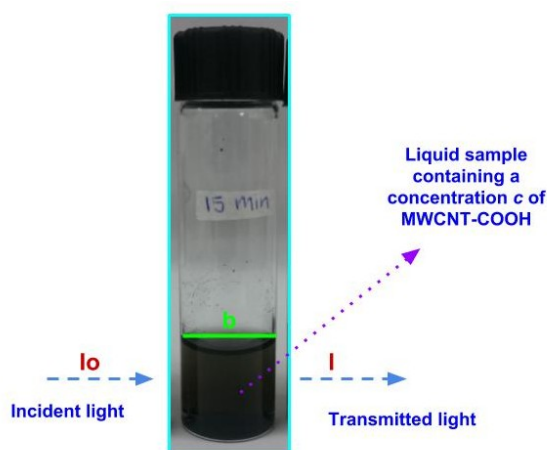


Figure 3.2: The process of transmittance for a solution formulated by dispersing a certain concentration c (wt%) of MWCNT-COOH in distilled water is showed. The beam of incident radiation (I_0) penetrates the first glass wall, passes through the solution which has a thickness of b (cm) and a concentration c (wt%) of MWCNT-COOH, the absorbing species, and is reflected with intensity (I) through the second glass. Due to the interactions between the photons of the incident radiation beam and the absorbent particles, the beam power is reduced.

According to Brunatti and Martín color helps to identify chemical substances by using detectors that measure its absorption, not only in the area of the visible spectrum, but also in ultraviolet and infrared.⁴¹ Spectrophotometry allow us to determine the amount of radiant energy absorbed by a chemical system as a function of the wavelength of radiation.⁴¹

Figure 3.2 shows the transmittance phenomenon for a solution formulated by dispersing a certain concentration

c (wt%) of MWCNT-COOH in distilled water. The beam of incident radiation penetrates the first glass wall, passes through the solution which have a thickness of b (cm) and a concentration c (wt%) of MWCNT-COOH, the absorbing species, and is reflected through the second glass. Due to the interactions between the photons of the incident radiation beam and the absorbent particles, the beam power is attenuated. Then, we can define the transmittance T of the solution as the fraction of the incident radiation transmitted by the solution,⁴¹

$$T = \frac{I}{I_o} \quad (3.1)$$

The absorption of light by atoms determines atomic absorption. As mentioned earlier, atoms absorb light at a defined wavelength.⁴⁰ For example, in aqueous solution, the wavelength of absorption for completely dispersed CNTs appears at 253 nm.⁴² Other studies indicate that the wavelength of absorption of nanotubes appears in the 200-1200 nm region.⁴³ In the case of MWCNTs and SWCNTs, their peaks of absorption appear at 253 nm, and 972 and 1710 nm, respectively.^{39, 43} As it was mentioned, the phenomena of absorption occurs when light at an specific wavelength has adequate energy to excite electrons to another electronic state. The absorbance of the solution represented in figure 3.2 is expressed as:

$$A = -\log T = \log \frac{I_o}{I} \quad (3.2)$$

Absorption spectroscopy in the ultraviolet (UV) and visible (Vis) range is important since the energy differences corresponds to those of the electronic states of atoms and molecules.⁴⁴ In the case of CNTs, UV-Vis spectroscopy quantifies nanotube dispersion properties by applying a light source on the suspension and correlating the amount of light absorbed or scattered with particle size in liquid samples.³⁹

3.1.2 Transmittance and Absorbance Measurements

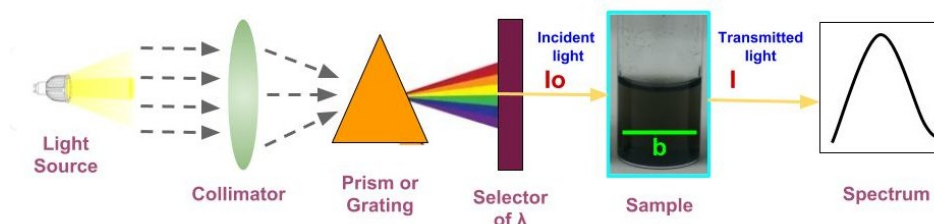


Figure 3.3: Process of transmittance and absorbance measurements. Diagram of a basic spectrometer formed by the source of radiation (light source). When radiation is emitted by the source, a portion of it is collected by a collimator and directed to the selector that transmits an specific range of wavelength to the sample. Once light, with intensity I_0 , reaches the sample, part of it is absorbed and the other is transmitted with intensity I . The fraction of light that is transmitted is caught by the detector which allows to analyze and plot the transmittance of light.

Transmittance and Absorbance are measured with an spectrophotometer.⁴¹ Figure 3.3 shows the scheme of a basic spectrometer. An spectrophotometer is former by the source of radiation. The source of radiation is usually tungsten or tungsten-halogen lamp to provide continuous radiation from the visible spectrum to the near infrared. In order to radiate ultraviolet light, a H_2 or D_2 lamp is needed.⁴⁵ When radiation is emitted by the source, a portion of it is collected and directed to the selector that transmits an specific range of wavelength to the sample.⁴⁵ Once light reaches the sample, part of it is absorbed and the other is transmitted. The fraction of light that is transmitted is caught by the detector.⁴⁵

A UV-Vis spectrometer uses the basic concepts presented in the previous subsection to measure the quality of dispersion of a liquid sample. In the case of an UV-Vis spectrometer, it uses the ultraviolet-visible-near-infrared region to collect information about absorption and transmittance of a liquid sample.³⁹ In the particular case of CNTs, the solution turns darker and absorbs more light as nanotubes are dispersed. The wavelength for completely dispersed CNTs appears in the 200 to 1200 nm region.³⁹ Other studies indicate that MWCNTs show a peak of absorption at 253 nm, while SWCNTs showed peaks of absorption at 972 nm, and 1710 nm.⁴³ In addition, some authors have suggested that maximum UV-Vis absorbance is a good indicator of maximum dispersion.⁴⁶

3.2 pH Analysis

In section 2.1.4, it was mentioned that the variation of the pH can cause the sedimentation of the particles and the perforation of the material. For this reason, the control of the pH is very important during the formulation of drilling fluids. So, what is the pH and how it is measured? In this section, the main principles of pH measurements are introduced.

The term pH is defined as the hydrogen ion activity or the effective concentration of hydrogen ion (H^+) in a solution. That is, the pH of a substance is a measurement of its acidity or basicity.⁴⁷ In order to understand the influence of pH in a solution, let's take a moment to review about acids and bases in aqueous solutions.

According to McMurry and Castellion in their book "*Fundamentals of General, Organic, and Biological Chemistry*", an acid is a substance that gives hydrogen ions, H^+ , when dissolved in water. On the other hand, a base is a substance that gives hydroxide ion, OH^- , when dissolved in water.⁴⁸ For a particular concentration of hydrogen ions (H^+), there is a corresponding concentration of hydroxyl ions (OH^-). This relationship results in equilibrium.¹⁴

In mathematical form, the pH scale is expressed as follows:

$$pH = -\log_{10}a_{H^+} \quad (3.3)$$

or,

$$10^{pH} = a_{H^+} \quad (3.4)$$

In the previous expressions, (a_{H^+}) represents the activity of the hydrogen ion which can be defined by using a relation between the concentration or molality (C_{H^+}) and the activity coefficient (f_{H^+}) as follows:⁴⁷

$$a_{H^+} = f_{H^+}C_{H^+} \quad (3.5)$$

A pH scale provide a range of acidity and basicity based on the dissociation constant for water, K_w .⁴⁷ The scale is divided in acid, neutral, and basic pH. For pure water, hydrogen ion (H^+) and hydroxyl ion (OH^-) concentration are equal to 10^{-7} M at ambient temperature. This measurement corresponds to neutral solution or neutral pH.⁴⁸ For acid and basic pH, the values of 0 and 14 were defined, respectively. Thus, the pH scale is defined with the following range: **a**) acidic solution ($pH < 7$), **b**) neutral solution ($pH = 7$), and **b**) basic solution ($pH > 7$).⁴⁸

3.2.1 Experimental Determination of pH



Figure 3.4: pH scale of the simplest method to measure pH. The method consists of a dye that changes color depending on the pH of the solution.

Figure 3.4 shows the one of the method to measure pH. The method consists in the use of an *acid-base indicator* which contains a dye that changes its color depending on the pH of the solution.⁴⁸ The measurement is carried out by putting a drop of solution on the paper and comparing the color resulting on the calibration chart. The calibration chart contains the pH scale with numbers from 0 to 14 and each number indicate a variety of colors. Once the colors of the measured sample are determined, the value of pH can be determined, too.

3.3 Rheology: Basic Concepts

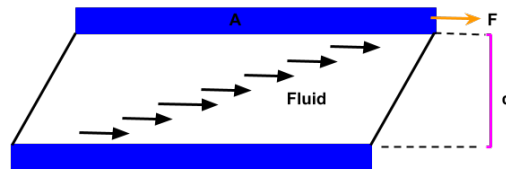


Figure 3.5: Two parallel planes of area A representing viscosity. The space between plates is filled with liquid. The upper plane moves with relative velocity U .

As mentioned in section 2.1.4, viscosity, thixotropy, pH, density, solid content, and mud-cake thickness are the main control parameters to characterize drilling fluids as optimal fluids during a drilling process. Rheology allows to study these parameters in order to determine their behavior. Since the purpose of this work is to study the influence of MWCNT-COOH on the behavior of viscosity at different temperatures, some basic and necessary concepts related to rheology will be explained briefly in this section.

First of all, rheology means the study of the deformation and flow of matter.⁴⁹ The flow behavior of ideally viscous liquids can be described under Newton's laws. Newton proposed that *"the resistance which arises from the lack of slipperiness of the parts of the liquid is proportional to the velocity with which the parts of the liquid are separated from one another"*.⁴⁹

In the previous paragraph, an important parameter was introduced; viscous liquid. When two solid bodies in contact move relative to each other, a friction force is generated at the contact surface in the opposite to the motion. This situation is similar when fluids moves relative to each other. In the particular case of fluids, the internal friction or resistance to flow is called viscosity.¹⁵

Barnes et al. define viscosity as the lack of slipperiness, internal friction, or the resistance to flow.⁴⁹ The deformation of a fluid can be described by two parallel plates separated by some distance as seen in figure 3.5. With the mentioned figure, we can obtain the mathematical relation for viscosity.¹⁴

The force per unit area required to produce motion, also called **shear stress**, is defined as F/A and is denoted by τ .⁴⁹ The mentioned force causes the layers to slide pass one another.¹⁴ The shear stress is proportional to the velocity gradient usually written as $\dot{\gamma}$ and also called **shear rate** U/d .⁴⁹ There also exists a viscosity coefficient denoted as η .

In a system like the one illustrated in the figure 3.5, the application of a shear stress τ generates the flow of liquid.⁴⁹ Thus,

$$\tau = \eta \cdot \frac{U}{d} \quad (3.6)$$

or,

$$\tau = \eta \cdot \dot{\gamma} \quad (3.7)$$

Equation 3.7 will be useful during the analysis of viscosity carried out in chapter five.

Cengel and Cimbala mention that fluids for which the rate of deformation is linearly proportional to the shear stress are called Newtonian fluids.¹⁵ Sanchez C. mentions that viscosity of a Newtonian fluid can vary with temperature and pressure, but it does not vary with the shear rate and time.³ Most common fluids such as water, alcohol, gasoline and light oils are Newtonian fluids.¹⁴ On the other hand, if the rate of deformation is not linearly proportional to the shear stress, fluids are called non-Newtonian. In the case of non-Newtonian fluids, viscosity varies by changes in temperature, pressure, shear rates and time.³ Some examples of non-Newtonian fluids are blood and liquid plastics.¹⁵

3.3.1 Parameters Affecting Viscosity

Yadav et al. mention that parameters affecting the viscosity are: temperature of the solution, pH of the solution, ionic strength of the solution, the velocity gradient under which viscosity coefficient was measured, concentration of the solute, among others.⁵⁰ Another study carried out by Sanchez C., mentions that viscosity can be influenced by six parameters: solute concentration of the drilling fluid, the temperature at which the fluid is exposed, the pressure that compresses the fluid and increases the intermolecular resistance, the shear rate, the time during which the material is subject to the shear rate, and the electric field that acts on the flow.³

3.3.2 Rheological Analysis

An important tool to investigate the rheological behavior of fluids is the rheometer. To perform the measurements required in this project, an hybrid rheometer model DHR, Discovery Hybrid Rheometer manufactured by TA Instruments, will be used. Figure 3.6 shows the model of the rheometer that will be used. The rheometer is complemented with an standard Peltier Concentric Cylinder geometry which include a cup radius of 15 mm, configured with a DIN Rotor.⁵¹

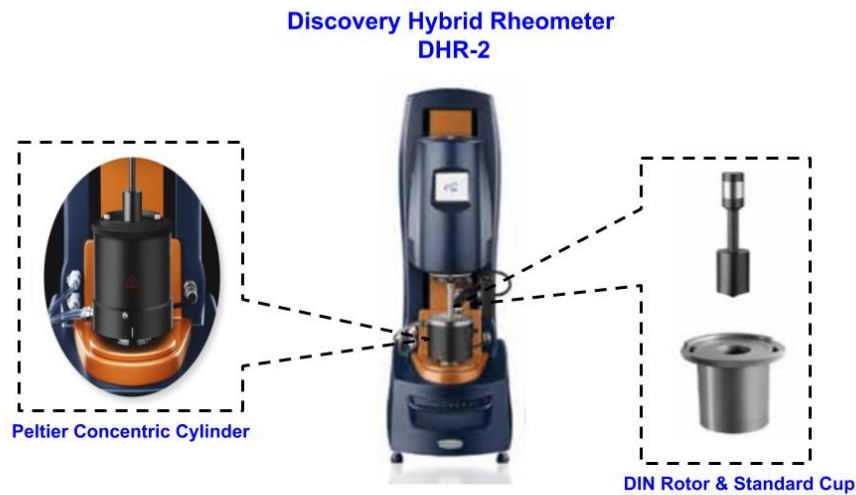


Figure 3.6: Model of a DHR rheometer and its main parts, the Peltier Concentric Cylinder configured with a DIN Rotor. Image adapted. Original Image: Reference [51]

Figure 3.7 shows the Peltier Concentric Cylinder. It controls the temperature system of the rheometer. It also has a Lower Cup Geometry which contains the sample during the measurements. The Peltier Concentric Cylinder works for a variety of cup and rotor geometries and it has four Peltier heating elements which offers a temperature range of -20°C to 150°C , with a maximum heating rate up to $13^{\circ}\text{C}/\text{min}$. Temperature is controlled with a platinum resistance thermometer (PRT).⁵¹

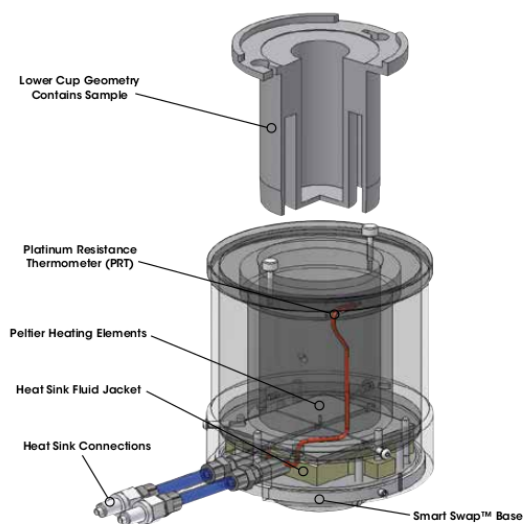


Figure 3.7: Peltier Concentric Cylinder System. Image Source: Reference [51]

It is important to mention that a DIN rotor will be used to perform measurements in the present project because of the low viscosity behavior of samples. The rotor has a radius of 14 mm and a height of 42 mm. Additionally, the equipment possess a Solvent Trap which includes a base reservoir Two-Piece Cover that is mounted to the shaft of the rotor providing a vapor barrier to seal the environment inside the cup and prevents solvent evaporation.⁵¹

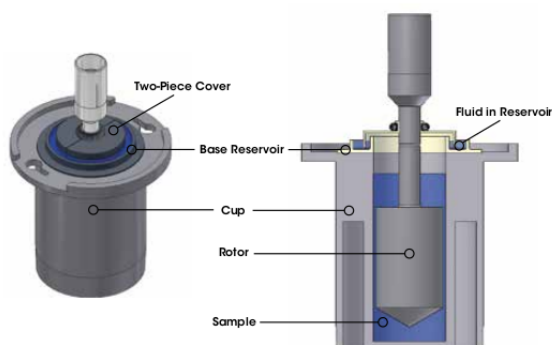


Figure 3.8: Peltier Concentric Cylinder System with a DIN rotor. Image Source: Reference [51]

Chapter 4

Methodology

4.1 Formulation of MWCNT-COOH Dispersions for Absorption Tests

4.1.1 Material Selection

To formulate the samples for the first part of the present research project, multi-walled carbon nanotubes functionalized with carboxylic acid (MWCNT-COOH) were used. In addition, distilled water was used. The pH of distilled water was approximately 7. It is important to mention that the functionalization of the MWCNT-COOH was not carried out during this project.

4.1.2 Sample Preparation

Five samples were prepared in order to study the dispersion of nanotubes. The five samples were obtained by mixing MWCNT-COOH at a concentration of 0.02 wt% with respect to 10 ml of distilled water. As mentioned in chapter three, a proper ultrasonication procedure often results in well-dispersed nanotubes and better composite mechanical properties.³⁹ Thus, in order to achieve an optimal dispersion of MWCNT-COOH, samples were ultrasonicated using a Bandelin Sonicator, operating at 75% of its total power (230V-50/60 Hz.) and pulses of 00.5; 00.1 s. The sonication process was carried out five times in order to find the optimal dispersion conditions (see table 4.1). In addition, each sample was sonicated by placing the vial inside a bath of ice water in order to prevent rising of the temperature.

Designation	Volume of Distilled Water (ml)	MWCNT-COOH Concentration (wt%)	Sonication Time (min)
A-1	10	0.02	5
B-1	10	0.02	10
C-1	10	0.02	15
D-1	10	0.02	20
E-1	10	0.02	30

Table 4.1: Synthesis of MWCNT-COOH dispersions.

Figure 4.1 shows the samples prepared during the synthesis of the five samples detailed in table 4.1.

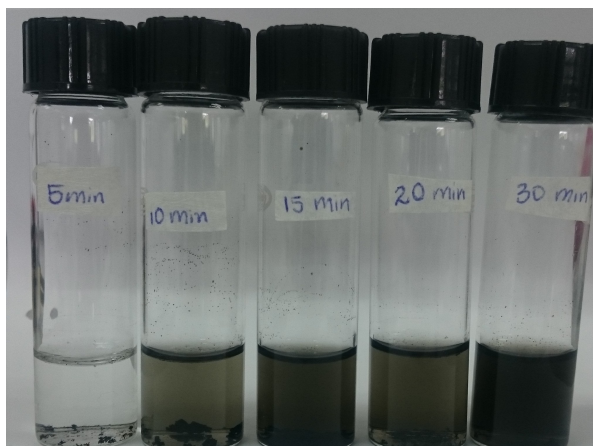


Figure 4.1: Samples prepared during the synthesis of MWCNT-COOH dispersions

4.1.3 Absorption Measurements

The absorption spectrum for samples detailed in table 4.3 was obtained with a UV-Vis spectrometer model Thermo Scientific NanoDrop 2000 operating between 100 to 900 nm. For more information about the principle of operation of the equipment refer to section 3.1.2.

4.2 Formulation of the Nano-Based Drilling Fluid

In this section, the materials used to carried out this research are presented. Also, the process for sample preparation and the protocols for the rheological measurements are explained.

4.2.1 Material Selection

Six samples were prepared (see Figure 4.2). The samples were prepared using distilled water ($\text{pH} \approx 7$), two different concentrations of MWCNT-COOH (0.01 wt% and 0.05 wt%), and Bentonite clays from tow different deposits: natural sodium bentonite from Ecuador and Peru. The nanotubes used in this section were described in section 4.1.1, during the formulation of nanotube dispersions for absorption tests.

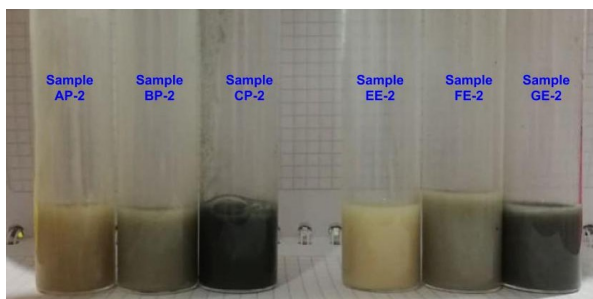


Figure 4.2: Samples prepared during the synthesis the nano-based drilling fluids.

4.2.2 Sample Preparation

Six samples were prepared using distilled water, natural sodium bentonite, and MWCNT-COOH. The protocol for the process of sample preparation was the following:

1. A solution containing distilled water and MWCNT-OOH at 0.1 wt% was prepared. This sample was formulated adding 0.175 g of MWCNT-COOH into 175 ml of distilled water. Then, the sample was ultrasonicated using a Bandelin Sonicator, operating at 75 % of its total power (230V-50/60 Hz.) and a pulse of 00.5; 00.1 s. In this case, the ultrasonication process was carried out during 30 minutes. This time was chose because it is the maximum time to achieve the most optimal dispersion (see chapter 5). In addition, the sample was sonicated by placing the vial inside a bath of ice water in order to prevent rising of the temperature.

2. 75 ml of the solution at 0.1 %wt were extracted from the total volume of solution prepared in step 1. Then, 75 ml of extra distilled water were added to the extracted volume. Thus, a solution with a total volume of 150 ml and a concentration of 0.05 %wt of MWCNT-COOH was obtained. Then, 50 ml of the solution at 0.05 %wt were extracted from the 150 ml and the remaining volume (100 ml) was divided into two equal parts. Thus, two solutions containing 50 ml of solution at 0.05 %wt were obtained. These two solutions were named CP-2 and GE-2, respectively.
3. From the remaining 50 ml in step 2, 20 ml were extracted. Then, 80 ml of extra distilled water were added to the extracted volume. Thus, 100 ml of solution at 0.01 wt% of MWCNT-COOH were obtained. The 100 ml were divided into two equal parts and two samples of 50 ml were obtained. The two samples were named BP-2 and FE-2, respectively.
4. Each of the samples prepared in steps 1. and 2. were subjected to a pH measurement in order to control the pH range required during the preparation of the drilling fluid. To carry out the pH measurement, pH paper was used. The paper was submerged in each of the dispersions. Then, the color obtained in the paper was compared with pH scales. As can be seen in the following table, all the samples had a pH of 8.

Designation	Distilled water (ml)	MWCNT-COOH (wt%)	pH
A-2	50	0.00	8
B-2	50	0.01	8
C-2	50	0.05	8
E-2	50	0.00	8
F-2	50	0.01	8
G-2	50	0.05	8

Table 4.2: Synthesis of MWCNT-COOH Dispersion to Formulate the NBDFs.

5. Once the six dispersions were prepared, 2 g of Peruvian sodium bentonite were added to samples A-2, B-2, and, C-2. Other 2 g of Ecuadorian sodium bentonite were added to the remaining 3 dispersions, samples E-2, F-2, and G-2. Additionally, the bentonites were slowly added to the dispersions under constant stirring during one hour to avoid the aggregate form, and the temperature of the magnetic stirred was maintained at 0 °C.³
6. Finally, the pH of the samples was measured after adding the bentonite to each of the dispersions in order to

control the pH of the final fluid. All the samples had a $\text{pH} \approx 9$.

In the following table, the samples prepared in this section are summarized.

Designation	Distilled water (ml)	MWCNT-COOH (wt%)	Bentonite (g)	Sonication Time (min)
AP-2	50	0.00	2	60
BP-2	50	0.01	2	60
CP-2	50	0.05	2	60
EE-2	50	0.00	2	60
FE-2	50	0.01	2	60
GE-2	50	0.05	2	60

Table 4.3: Formulation of the nano-based drilling fluid. Samples AP-2, BP-2, and CP-2 were prepared using Peruvian bentonite, while samples EE-2, FE-2, and GE-2 were prepared using Ecuadorian bentonite.

4.2.3 Rheological Measurements

In order to obtain valid results of the rheological behavior of the fluid, all samples are measured following the same conditions. The measurements were performed with an hybrid rheometer model DHR, Discovery Hybrid Rheometer. The rheometer was complemented with an standard Peltier Concentric Cylinder geometry which include a cup radius of 15 mm, configured with a DIN Rotor.⁵¹ Refers to section 3.3 for more information about the mentioned instrument.

On the other hand, two temperatures were chosen for the rheological analysis, 25°C and 50°C. As it was mentioned at the beginning of this work, the purpose of this project is to analyze the influence of carbon nanotubes over the rheological properties of the nano-based drilling fluid at ambient temperature and high temperature. All measurements were carried out for the mentioned two temperatures.

To establish the rheological measurement protocol, previous tests were performed. First, different shear rates were applied in order to determine the range of rates in which the viscosity increases, decreases, or remains constant. Thus, it was observed that the viscosity increases drastically at shear rates lower than 10 s^{-1} , and that reaches its steady state at shear rates higher than 40 s^{-1} . Second, the time necessary for the viscosity to reach its steady state was 25 s. Finally, once the first tests were completed, it was established that the rheological measurement protocol will be carried out in two ways: performing measurements of structural construction and performing measurements of structural destruction. The measurements were carried out by applying step jumps with progressive increase of

the shear rate.

Constructive Measurements

To analyze the constructive behavior of the material, step jumps between high and low shear rates were carried out. Therefore, a maximum shear rate was applied during 25 s, followed by a process of structural constructive at low shear rate.

In figure 4.3, the process of structural constructive is showed. As can be seen, the measurement start with the application of a maximum shear rate of 100 s^{-1} in order to depart from a destructured level of the material, followed by a minimum shear rate of 0.01 s^{-1} to allow the structural constructive of the material. The process continues with jumps of destruction between 100 s^{-1} , and progressive increasing values of shear rate to study the constructive behavior. Each jump was measured during 25 s, without rest time between each jump. This time was considered because it was the maximum time to reach a constant viscosity, or an equilibrium state of viscosity. Additionally, each measurement was carried out for three times in order to guarantee repeatability of the results.

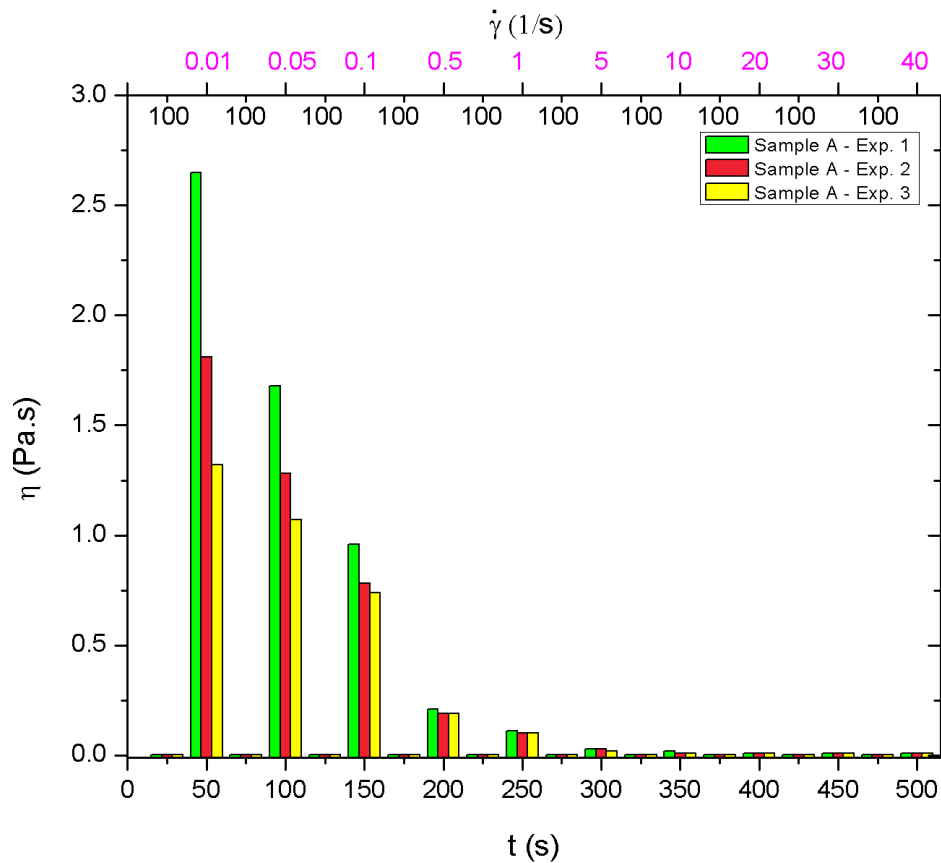


Figure 4.3: Measurement of the constructive behavior of the nano-based drilling fluid. The test consists of the application of a shear rate of 100 s^{-1} , followed by a shear rate of 0.01 s^{-1} . The process continues with jumps between 100 s^{-1} , and progressive increasing values of shear rate. Each jump was measured during 25 s.

Destructive Measurements

In the case of destructive measurements, step jumps between low and high shear rates were performed. A minimum shear rate was applied during 25 s, followed by a process of destruction at higher values of shear rate.

Similar to the structural constructive case, figure 4.4 shows the process of destruction of the material. As can be seen, the measurement start with the application of a minimum shear rate of 0.01 s^{-1} where the material is constructed structurally, followed by a shear rate of 0.05 s^{-1} . The process continues with jumps between 0.01 s^{-1} ,

and progressive increasing of shear rate values to analyze structural destructive and its influence over viscosity . Similarly to the constructive process, each jump was measured during 25 s. Additionally, each measurement was carried out for three times in order to guarantee repeatability of the results.

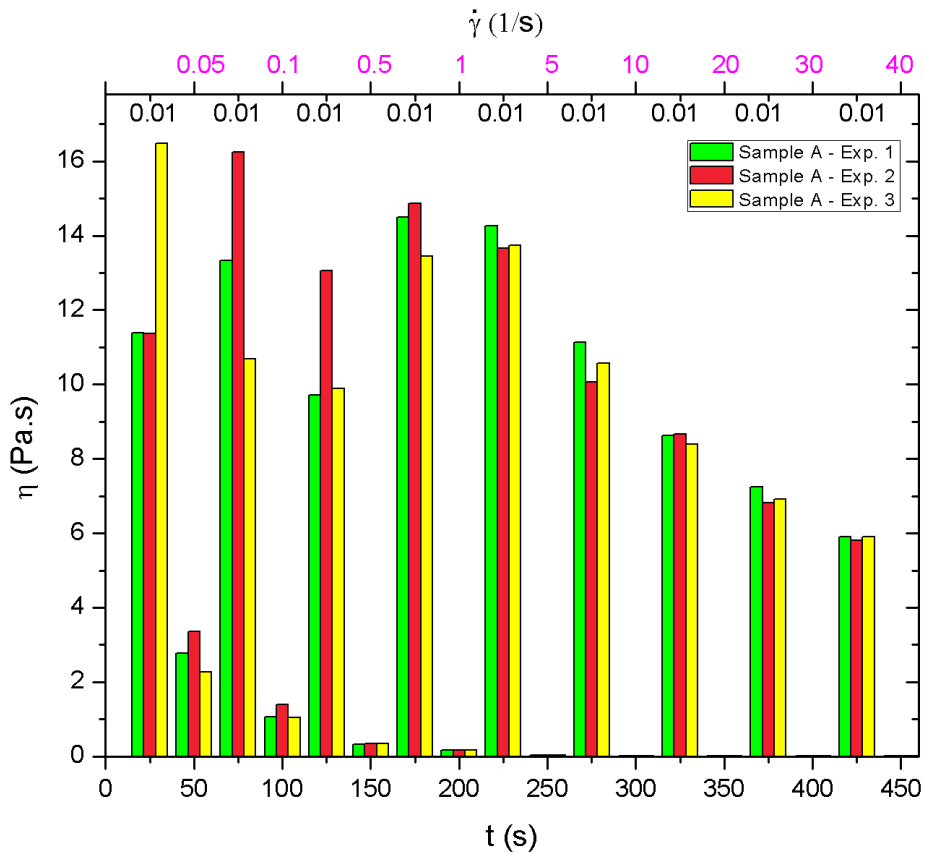


Figure 4.4: Measurement of the destructive behavior of the nano-based drilling fluid. The test consists of the application of a shear rate of 0.01 s^{-1} , followed by a shear rate of 0.05 s^{-1} . The process continues with jumps between 0.01 s^{-1} , and progressive increasing values of shear rate. Each jump was measured during 25 s.

Chapter 5

Results & Discussion

5.1 Absorption Analysis of MWCNT-COOH Dispersions

Once the samples formulated in section 4.1 were dispersed by ultrasonication for five different times, they were subjected to absorption measurements using a UV-Vis spectrometer. The data collected during the measurement indicated that the most optimal dispersion was achieved after 30 minutes of ultrasonication.

The UV-Vis spectrum presented in figure 5.1 shows the peaks of absorbance with respect to the wavelength absorbed by all the solutions of MWCNTs-COOH prepared in section 4.1. The spectrum was obtained at different ultrasonication times. As can be seen, it showed a maximum absorbance in a range of wavelengths between 200 and 300 nm. This result was consistent with outcomes found in literature, which indicate that the characteristic peak of absorption of MWCNT is located around 253 nm (see section 3.1.1).⁴²

As can be seen in figure 5.1, samples A-1, B-1, and C-1, which corresponds to ultrasonication times of 5, 10, and 15 minutes of ultrasonication, respectively, had a large amount of aggregates of nanotubes because the area of absorption is small. This observation is an indicator of low dispersion.³⁹ Comparing this result with the absorption peaks showed in figure 5.1, it can be noted that there was no absorption after 5 minutes of ultrasonication. Thus, the nanotubes were not optimally dispersed. In addition, the short area of absorption after 10 and 15 minutes of ultrasonication confirmed low dispersion of samples B-1 and C-1. However, an increment in the intensity of the peaks with time was observed. This result indicated that as the ultrasonication time increases, the aggregates of nanotubes dispersed due to the mechanical energy supplied was sufficient to break the van der Waals interactions.⁵² As a result, the absorbance increased.

In addition, as can be observed in figure 5.1, the increase of dispersed nanotubes resulted in an increase in the absorbance area. Thus, it was concluded that the larger the area under the absorbance curve, the greater and more optimal the dispersion of nanotubes was. Therefore, the most optimal sonication time for the preparation of samples in section 4.2 was 30 minutes. This result corresponds to sample E-1.

It is important to mention that before the measurements of the absorption spectrum of samples A-1, B-1, C-1, D-1, and E-1, a sample of distilled water was taken as the blank (reference sample). Therefore, the blank reading was treated as the new zero and the samples containing MWCNT-COOH were measured with respect to the blank. If the five samples have a higher level of analyte dispersed in water, then their absorbance will be positive. This result was observed for samples B-1, C-1, D-1, and E-1. On the other hand, if the five samples have a lower level of analyte dispersed in water, then their absorbance will be negative. This result was observed in sample A-1 which had a negative absorbance.

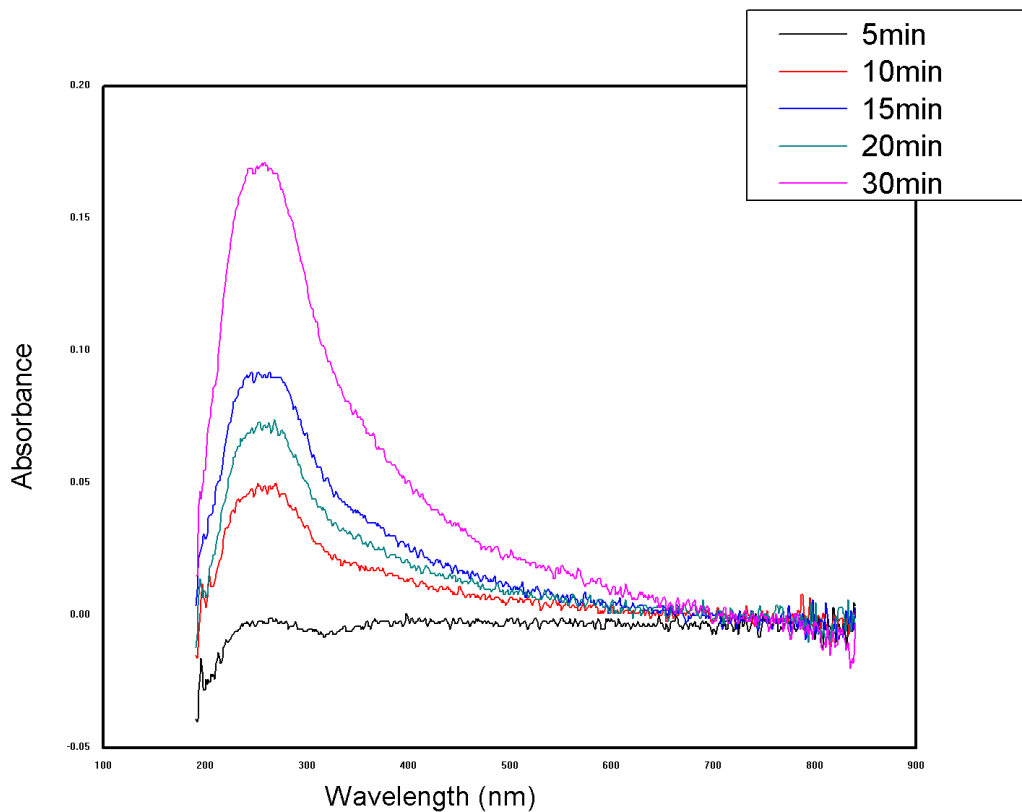


Figure 5.1: The peaks of absorption of MWCNT-COOH dispersions are showed. As can be seen, the peaks represent the samples ultrasonicated for five different times (5, 10, 15, 20, and 30 minutes). The peak of maximum absorption is located between 200 and 300 nm and it belongs to the sample sonicated during 30 minutes.

5.2 Rheological Analysis of the Nano-Based Drilling Fluid

5.2.1 pH Analysis

As it was mentioned in section 2.1.4, pH is one of the most important parameters of a drilling fluid. It is important to maintain a controlled pH because its change could modify the structure and the rheological behavior of the fluid.³. A

variation on the pH scale can cause sedimentation of the particles and the perforation of the material.³ In addition, the pH scale is one parameters that guarantee the use of the fluid during a drilling process because it helps with the mitigation of corrosion of the drill string.⁵³

According to Darley and Gray, in their book "*Composition and Properties of Drilling and Completion Fluids*", a mud made with bentonite and fresh water will have a pH between 8 to 9.⁵³ Other studies indicate that most water-based fluids are alkaline and work with a pH range between 7.5 to 11.5.⁴ Therefore, results showed in table 5.1, obtained during the measurement of pH of the nano-based drilling fluid, shows acceptable values of pH. Thus, the presented results determine that the addition of MWCNT-COOH do not affect significantly the pH of the nano-based drilling fluid.

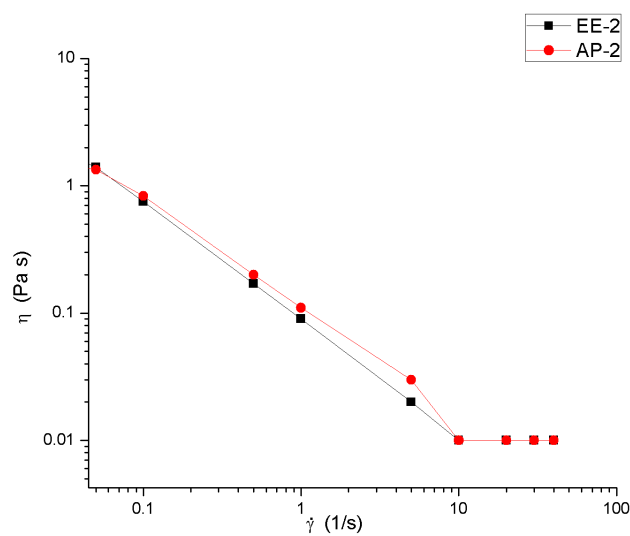
Designation	Distilled water (ml)	MWCNT-COOH (wt%)	Bentonite (g)	pH
AP-2	50	0.00	2	≈ 9
BP-2	50	0.01	2	≈ 9
CP-2	50	0.05	2	≈ 9
EE-2	50	0.00	2	≈ 9
FE-2	50	0.01	2	≈ 9
GE-2	50	0.05	2	≈ 9

Table 5.1: pH results obtained during the pH measurements of the nano-based drilling fluid.

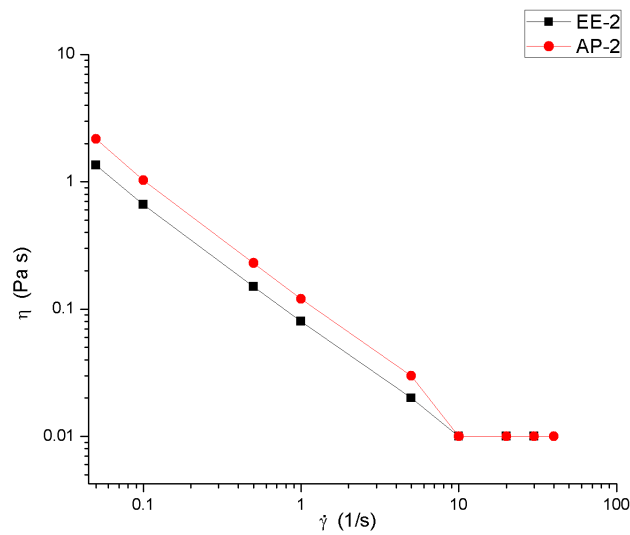
5.2.2 Viscosity Analysis

In order to determine the behavior of viscosity at different values of shear rates, a protocol for rheological measurements, detailed in section 4.2.3, was performed for each sample detailed in table 4.3. As mentioned in section 4.2.3, measurements were performed in two ways: first, the structural constructive behavior of the fluid as function of time was analyzed by applying step jumps between 100 s^{-1} and a progressive increase of the shear rate from 0.01 s^{-1} to 40 s^{-1} . In this way, 9 measurement points were obtained (see figure 5.2a). In the same way, the behavior of structural destructive as function of time was analyzed by means of the application of step jumps between 0.01 s^{-1} and a progressive increase of the shear rate from 0.05 s^{-1} to 40 s^{-1} (see figure 5.2b). Thus, 9 measurement points were obtained. All the samples detailed in the table 4.3 were submitted to the mentioned measurements. The time for structural constructive and destructive for each jump was 25 s, with no resting time between jumps. Additionally, it is important to mention that each measurement was repeated three times, under the same conditions,

and an average of viscosity was calculated. The averaged viscosity was chosen to plot results. Also, both methods were applied for two different temperatures, 25°C and 50°C. Once this is explained, the results obtained during the rheological experimentation are presented below. Also, results are going to be presented as a comparison between different concentration of MWCNT-COOH for each type of bentonite, Ecuadorian and Peruvian.

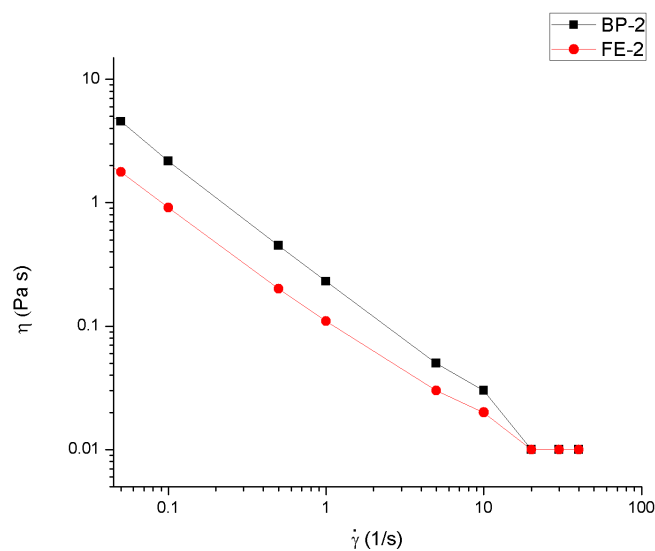
Structural Constructive and Destructive Analysis at 25°C

(a) Structural Constructive

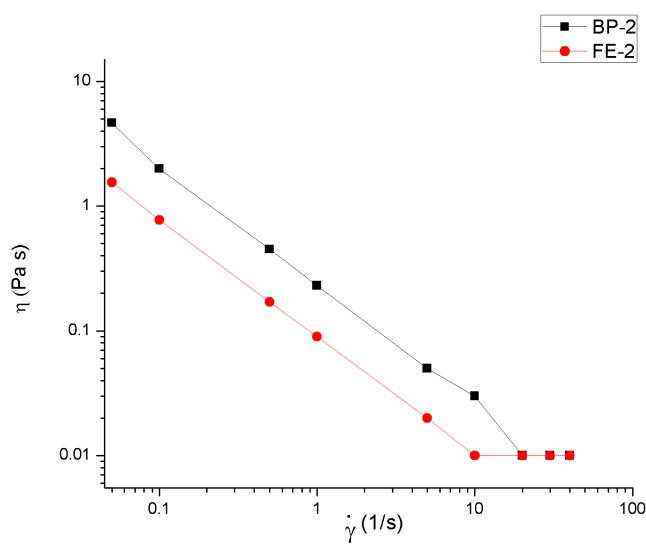


(b) Structural Destructive

Figure 5.2: Structural constructive and destructive analysis of samples AP-2 and EE-2. Both samples contain 0 wt% of MWCNT-COOH. Measurements were performed at room temperature, 25°C.

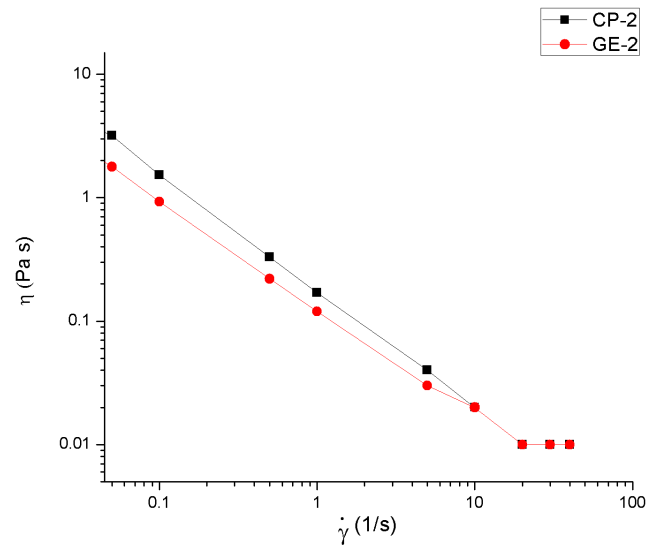


(a) Structural Constructive

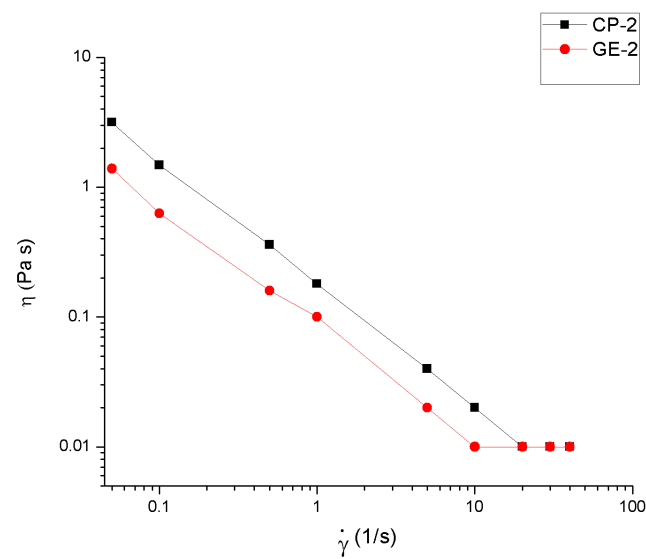


(b) Structural Destructive

Figure 5.3: Structural constructive and destructive analysis of samples BP-2 and FE-2. Both samples contain 0.01 wt% of MWCNT-COOH. Measurements were performed at room temperature, 25°C.



(a) Structural Constructive



(b) Structural Destructive

Figure 5.4: Structural constructive and destructive analysis of samples CP-2 and GE-2. Both samples contain 0.05 wt% of MWCNT-COOH. Measurements were performed at room temperature, 25°C.

Results presented in figure 5.2 show the behavior of viscosity during the structural constructive and destructive analysis of the material at room temperature. The constructive analyzes of samples EE-2 and AP-2, showed similar values of viscosity. However, during the process of structural destructive, the viscosity of sample AP-2 elaborated with Peruvian bentonite was greater than the viscosity of sample EE-2 elaborated with Ecuadorian bentonite.

In the structural destructive protocol presented in section 4.2.3, the range of shear rates started from 0.05 s^{-1} to 40 s^{-1} , and between each increment of shear rate, a minimum shear rate of 0.01 s^{-1} was applied. When shear rates started to increase progressively, the viscosity started to decrease with time until reaching its point of stability. According to literature, when a high shear rate is applied, particles suspended in the liquid rotate along in the flow direction, then they are oriented, deformed, disaggregated, and homogenized. While at rest, that is, at minimum shear rates such as 0.01 s^{-1} , the particles will maintain an irregular internal order and, consequently, they will have a considerable internal resistance against the flow, that is, a high viscosity.⁵⁴

Results showed in the figure 5.2 were consistent with the aforementioned. That is, at very low shear rates viscosity increased drastically. While at high speeds, viscosity remained constant. The same behavior was observed in samples BP-2, CP-2, FE-2, and GE-2 showed in figures 5.3 and 5.4. However, the difference in viscosity was much more appreciable compared to samples AP-2 and EE-2. Additionally, it was observed that viscosity of samples BP-2 and CP-2 prepared with Peruvian bentonite was greater than viscosity of samples FE-2 and GE-2 formulated with Ecuadorian bentonite, this result could be attributed to better absorption properties of Peruvian bentonite. This behavior was appreciated during the structural constructive and destructive analysis.

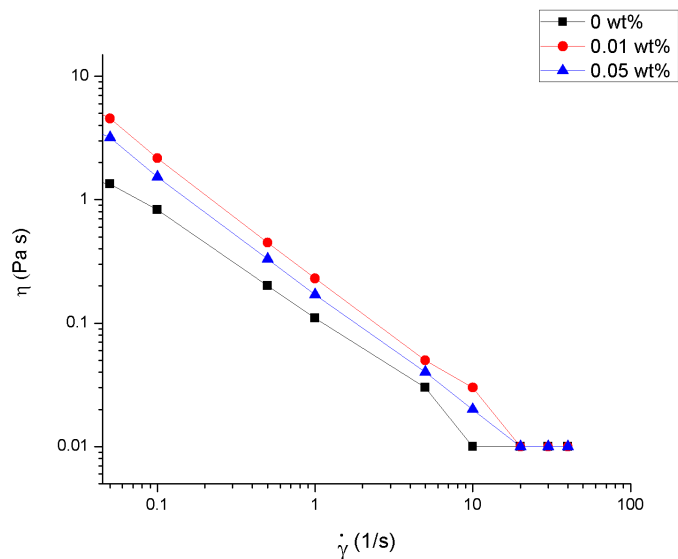
In section 3.3, the concept of viscosity of a Newtonian and non-Newtonian fluid was explained. It was mentioned that the viscosity of a Newtonian fluid remains constant regardless of the shear stress or the applied shear rate. On the other hand, the viscosity of a non-Newtonian fluid varies with changes in temperature, pressure, shear stress and shear rate.³ Taking into account this details, results observed in figures 5.2, 5.3, and 5.4 allowed to characterize all the measured samples as fluids with non-Newtonian viscosity at shear rates lower than 10 s^{-1} , while at speeds higher than 10 s^{-1} , where the viscosity remained constant, the samples acquired a Newtonian behavior.

5.2.3 Viscosity vs. Concentration of MWCNT-COOH

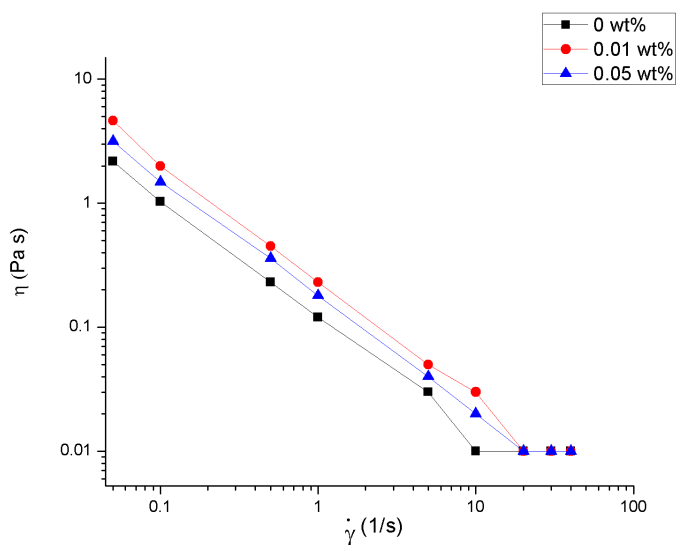
In the following table, results of viscosity are showed. The result were obtained from measurements of structural destructive and constructive at room temperature.

Designation	MWCNT-COOH (wt%)	Viscosity in Construction (Pa-s)	Viscosity in Destruction (Pa-s)
AP-2	0.00	1.93	2.17
BP-2	0.01	13.54	4.64
CP-2	0.05	7.87	3.16
EE-2	0.00	3.76	1.35
FE-2	0.01	5.85	1.55
GE-2	0.05	5.96	1.39

Table 5.2: Maximum values of viscosity reached by each sample during structural constructive and destructive at 25°C

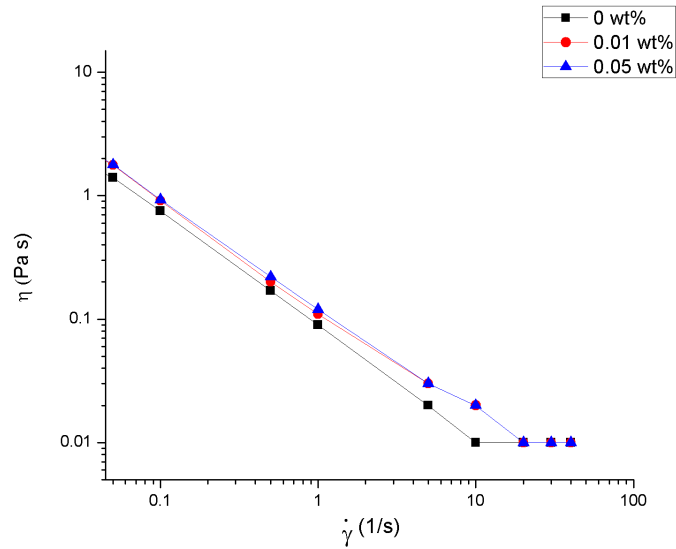


(a) Structural Constructive

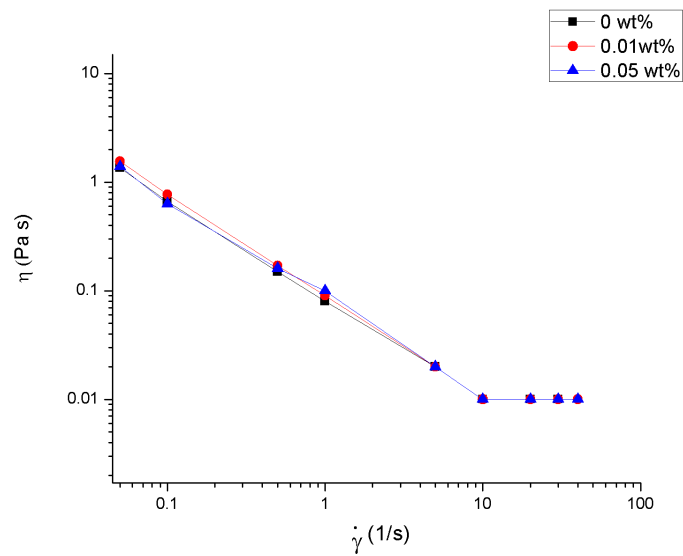


(b) Structural Destructive

Figure 5.5: Structural constructive and destructive analysis of samples AP-2, BP-2 and CP-2. The three samples were prepared using Peruvian bentonite. Also, sample AP-2 was prepared without MWCNT-COOH. While samples BP-2 and CP-2 were prepared using 0.01 wt%, and 0.05 wt% of MWCNT-COOH, respectively. Measurements were performed at ambient temperature, 25°C.



(a) Structural Constructive



(b) Structural Destructive

Figure 5.6: Structural constructive and destructive analysis of samples EE-2, FE-2 and GE-2. The three samples were prepared using Ecuadorian bentonite. Also, sample EE-2 was prepared without MWCNT-COOH. While samples FE-2 and GE-2 were prepared using 0.01 wt%, and 0.05 wt% of MWCNT-COOH, respectively. Measurements were performed at ambient temperature, 25°C.

Several studies were performed to study the effect of carbon nanotubes over the rheological properties of drilling fluids. According to Ismail et al. a small concentration of MWCNT causes an increase of viscosity in the fluid.¹ This was evidenced in the results obtained in figure 5.5, for the samples containing different concentration of MWCNT-COOH.

Figure 5.5 shows the results of viscosity obtained for composites formulated with Peruvian bentonite. As can be seen, sample BP-2 which contain 0.01 wt% of MWCNT-COOH had higher viscosity than samples AP-2 and CP-2, which contain 0 wt% and 0.05 wt% of MWCNT-COOH, respectively (see table 5.2). Ismail et al. mention that the addition of MWCNT to the drilling fluid increases the volume concentration of solids due to the huge surface area to volume ratio that MWCNT possesses.¹ In addition, an study performed by Sanchez C.³ reported that an increase in the volume concentration of solids in bentonite suspension causes the increase of viscosity. Thus, the increase in viscosity of sample BP-2 and CP-2 in figure 5.5 could be attributed to the increase of the volume concentration of solids in the composite.

In contrast with samples formulated with Peruvian Bentonite, the process of structural constructive of samples EE-2, FE-2, and GE-2 did not show a significant change in viscosity. However, according to values presented in table 5.2, the higher viscosity was achieved by sample GE-2, which contain the higher concentration of MWCNT-COOH (0.05 wt%). In the case of structural destructive, results in table 5.2 showed similar values of viscosity.

Comparing results of structural constructive presented in table 5.2, sample AP-2, formulated with Peruvian bentonite, showed lower viscosity than sample EP-2, formulated with Ecuadorian bentonite. Both samples do not contain MWCNT-COOH. However, when a little amount of MWCNT-COOH was added to the composites, samples formulated with Peruvian bentonite (BP-2 at 0.01 wt%, and CP-2 at 0.05 wt%) showed higher viscosity than samples formulated with Ecuadorian bentonite (FE-2 at 0.01 wt% and GE-2 at 0.05 wt%). On the other hand, comparing results of structural destructive, it can be noted that samples formulated with Peruvian bentonite showed higher viscosity than samples formulated with Ecuadorian bentonite. As conclusion, it can be noted that samples prepared with Peruvian bentonite required less concentrations of MWCNT-COOH to have changes in the viscosity than samples prepared using Ecuadorian bentonite.

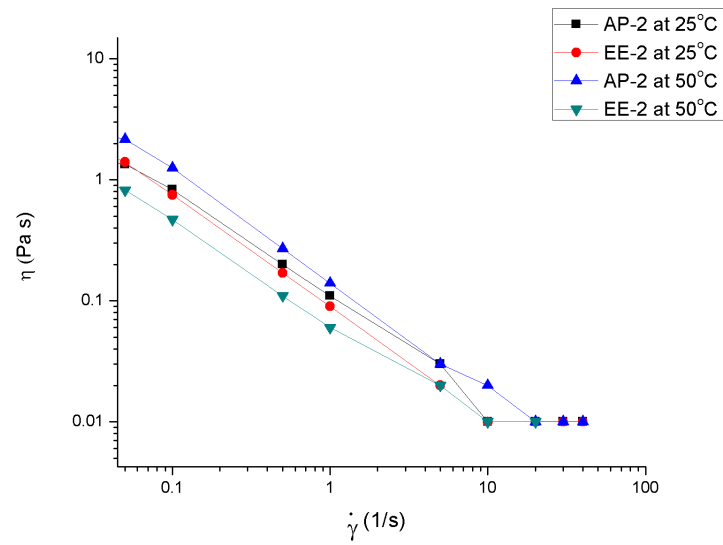
5.2.4 Viscosity vs. Temperature

In this section, the influence of temperature over the rheological behavior of viscosity is presented. The results reported in this section were obtained following the protocol of structural constructive and destructive analysis detailed in section 4.2.3. In this case, the temperature was risen to 50°C in order to analyze the influence of

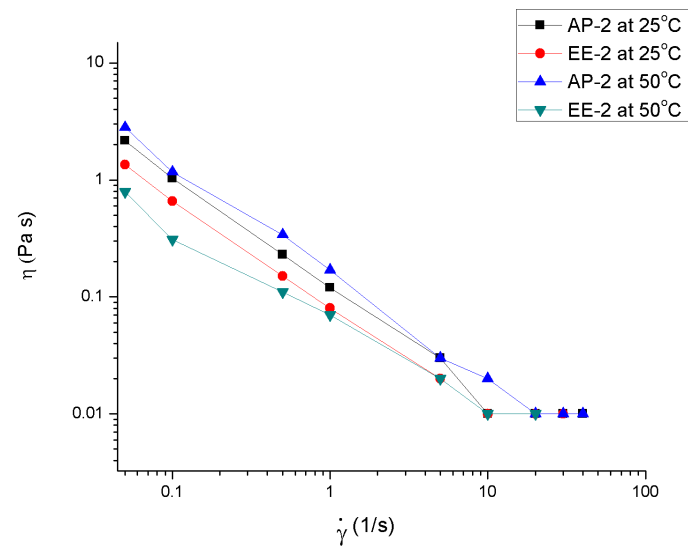
MWCNT-COOH on the behavior of viscosity. In the following table, results of viscosity are showed.

Designation	MWCNT-COOH (wt%)	Viscosity in Construction (Pa-s)	Viscosity in Destruction (Pa-s)
AP-2	0.00	3.43	2.81
BP-2	0.01	14.34	4.18
CP-2	0.05	8.07	3.14
EE-2	0.00	2.01	0.79
FE-2	0.01	6.25	1.31
GE-2	0.05	9.67	2.28

Table 5.3: Maximum values of viscosity reached by each sample during structural constructive and destructive analysis at 50°C

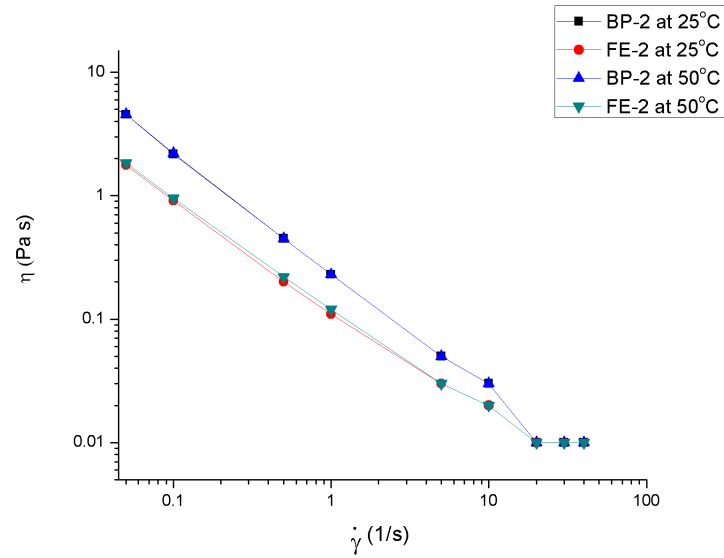


(a) Structural Constructive

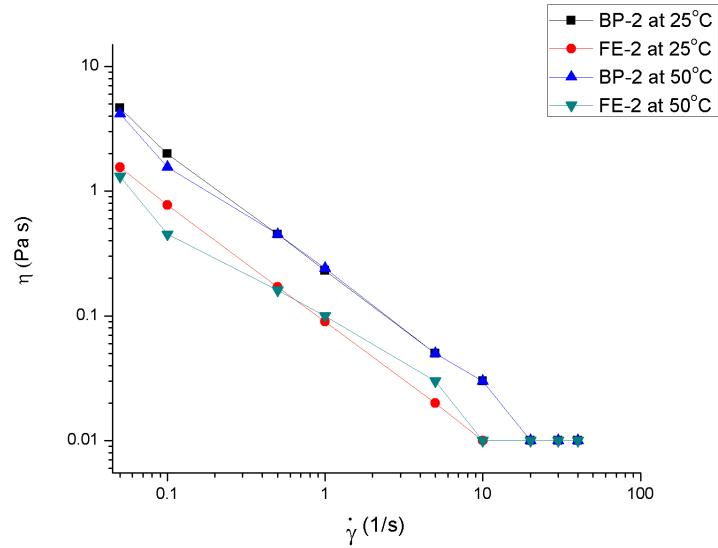


(b) Structural Destructive

Figure 5.7: Comparison of the results of structural constructive and destructive analysis of samples AP-2 and EE-2, formulated with 0.00 wt% of MWCNT-COOH, at 25°C and 50°C.

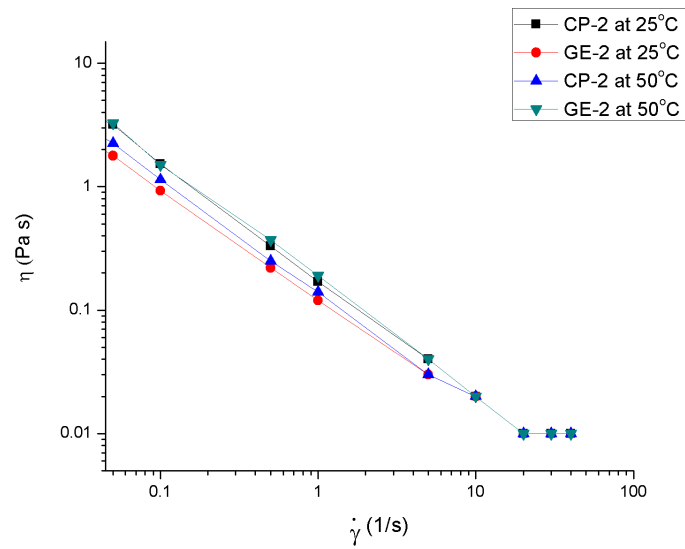


(a) Structural Constructive

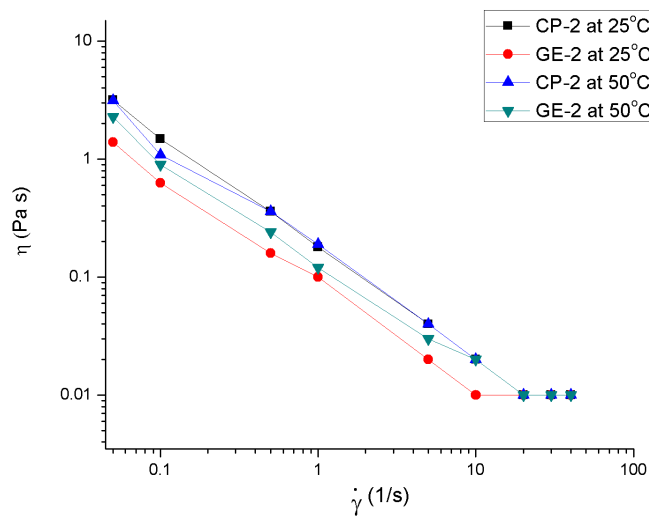


(b) Structural Destructive

Figure 5.8: Comparison of the results of structural constructive and destructive analysis of samples BP-2 and FE-2, formulated with 0.01 wt% of MWCNT-COOH, at 25°C and 50°C.



(a) Structural Constructive



(b) Structural Destructive

Figure 5.9: Comparison of the results of structural constructive and destructive analysis of samples CP-2 and GE-2, formulated with 0.05 wt% of MWCNT-COOH, at 25°C and 50°C.

Several studies have reported results about the influence of carbon nanotubes over the rheological properties of drilling fluids at high temperature conditions. Ismail et al. mention that a little concentration of MWCNT increases the plastic viscosity at 27°C, 138°C, and 193°C.¹ Results presented in figure 5.7, showed the behavior of samples AP-2 and EE-2, both samples were formulated without MWCNT-COOH. As can be noted, the viscosity of sample AP-2, formulated with Peruvian bentonite, increased approximately twice during the structural constructive study at 50°C. However, during the destructive analysis, the viscosity remained without significant changes. On the other hand, the viscosity of sample EE-2, formulated with Ecuadorian bentonite, decreased approximately twice during the structural constructive and destruction analysis at 50°C. To sum up, viscosity of sample AP-2 prepared with Peruvian bentonite increased with temperature, and viscosity of sample EE-2 prepared with Ecuadorian bentonite decreased.

Different results are showed in figure 5.8 and 5.9. Samples BP-2 and CP-2, formulated with Peruvian bentonite and with 0.01 wt%, and 0.05 wt% of MWCNT-COOH, respectively, did not show changes in viscosity during structural constructive and destructive analysis at high temperature. This can be attributed to the high thermal conductivity of carbon nanotubes when supporting high temperature conditions.³⁴ This result could be an advantage during the process of drilling at extreme conditions of temperature. On the other hand, samples FE-2 and GE-2, formulated with Ecuadorian bentonite, and with 0.01 wt%, and 0.05 wt% of MWCNT-COOH, respectively, had an increase on viscosity when temperature was increased. According to Goyal MK in his book "*Fluid Mechanics and Hydraulic Machines*"⁵⁵, when the temperature of a liquid increase, the viscosity decrease due to the reduction of the intermolecular cohesion. Contrary to Goyal MK., the results of viscosity obtained for samples AP-2, FE-2, and GE-2 showed an increasing of viscosity. This behavior may be attributed to the evaporation of water during the measurements, which increase the concentration volume of solid causing and increasing of viscosity.

From results obtained in figures 5.7, 5.8, and 5.9, it can be concluded that the addition of MWCNT-COOH controls the increasing of viscosity of composites when they are exposed to high temperatures. As mentioned at the beginning of this work, the motivation of this work is based on the use of the thermal properties of carbon nanotubes to control the rheological properties of drilling fluids at high temperatures. The results obtained in this report, confirm results presented in other studies. In addition, composites formulated with Peruvian Bentonite and MWCNT-COOH showed better control of viscosity at 50°C than composites formulated with Ecuadorian bentonite. This behavior could be attributed to chemical composition and particle size of bentonites.

As final discussion, it is important to mention that in a study carried out by Villaroel L.⁴ indicates the viscosity values obtained during a rheological study of a drilling fluid composed of calcium carbonate in order to minimize the damage in production formations in the Sacha field. In this study, Villaroel details the plastic viscosity values of the

fluid that will be used during the drilling process which was carried out by stages. For the first stage, of depth 5400 ft, a fluid with the minimum possible viscosity was required. The second stage, with a depth from 5400 ft to 8600 ft, required a fluid with a maximum viscosity of 0.03 Pa-s. The third and last stage, with a depth from 8600 ft to 10000 ft, required a fluid with a maximum viscosity of 0.03 Pa-s. The majority of fluids elaborated in the present work, showed viscosity values lower than 10 Pa-s which, in comparison with the viscosity values presented by Villaroel L., are high. However, the samples formulated with Ecuadorian bentonite showed the minimum viscosity values at room temperature in comparison with samples formulated with Peruvian bentonite, making them good candidates for the development of drilling fluids. On the other hand, samples prepared with Peruvian bentonite showed better control of viscosity at higher temperature.

Another study carried out by Sanchez C.,³ in which an analysis of suspensions of Peruvian sodium bentonite was carried out, indicates that the viscosity values for a suspension of 4 wt% of bentonite go from 1,038 Pa-s with a shear rate of 0.51 s^{-1} up to 0.053 Pa-s for a shear rate of 14 s^{-1} . That is, as the shear rate increases, the viscosity decreases. These relationship is similar to the relation obtained in this work, where the viscosity also decreased as shear rate increased. Additionally, in the present work in which concentrations of 4 wt% of bentonite were also used. Finally, the results obtained in this study indicate that the addition of MWCNT-COOH to bentonite suspension increases their viscosity. However, MWCNT-COOH maintains the viscosity stable at high temperature.

Chapter 6

Conclusions & Outlook

This chapter presents the conclusions and recommendations obtained during the development of this project. Taking into account each of the objectives proposed at the beginning of this work, the following conclusions are presented.

- Through a rheological study, the behavior of viscosity, at different temperatures, of a simple drilling fluid formulated using water, Peruvian and Ecuadorian bentonite, and multilayer carbon nanotubes was established.
- From an absorbance analysis, carried out with a UV-Vis spectrophotometer, the maximum absorption peak of the MWCNT-COOH was obtained. The maximum peak was located between 200 and 300 nm and corresponds to the sample E-1 which was ultrasonicated for 30 minutes. Thus, it is concluded that sample E-1 shows the most optimal dispersion of multilayer carbon nanotubes. In addition, it is established that the optimal time of ultrasonication to achieve an adequate dispersion of the nanotubes was 30 minutes.
- Through a pH study of the NBDF formulated in this project, it is concluded that the addition of low concentrations of MWCNT-COOH (0.01 and 0.05 wt%) maintains the pH range required for drilling fluids. The resulting pH of all NBDF samples was 8 ± 0.5 , which is within the basic pH range required.
- The rheological analysis carried out in this project, offers an analysis of the behavior of the viscosity of the NBDF samples through structural constructive and destructive measurements. With the results obtained in these measurements, it is concluded that at room temperature, the structural constructive process of the samples EE-2 and AP-2, which contains 0.00 wt% of MWCNT-COOH, show very similar viscosity values. Thus, there is no significant difference between the viscous properties of a fluid formulated with Peruvian bentonite and

a fluid formulated with Ecuadorian bentonite when high deformation rates (100 s^{-1}) are applied. However, during the process of structural destructive at low deformation rates (0.01 s^{-1}), the viscosity of sample AP-2 is greater than sample EE-2. When low concentrations of MWCNT-COOH are added to the fluid, the viscosity difference increases. The samples BP-2 and CP-2 formulated with Peruvian bentonite and 0.01 wt% and 0.05 wt%, respectively, have higher viscosity than the samples FE-2 and GE-2 formulated with Ecuadorian bentonite.

- The addition of low concentrations of MWCNT-COOH (0.01 wt% and 0.05 wt%) changes the behavior of the viscosity at different temperatures. In the case of the samples made with Peruvian bentonite it is observed that the samples BP-2, formulated with 0.01 wt% of MWCNT-COOH, show higher viscosity than the sample CP-2, formulated with 0.05 wt% of MWCNT-COOH. On the other hand, samples EE-2, FE-2, and GE-2 made with Ecuadorian bentonite did not show significant changes in viscosity.
- At high temperatures, the addition of low concentrations of MWCNT-COOH helps control the increase in viscosity. The samples elaborated with Peruvian bentonite and MWCNT-COOH showed better control of the increase in viscosity at 50°C compared to the results of the samples made with Ecuadorian bentonite. Therefore, Peruvian bentonite could be useful during drilling process due to the stability of viscosity at high temperatures.
- During the dispersion tests of the MWCNT-COOH, it is recommended to control the volume of sample to be ultrasound, since the greater the volume of the sample, the greater the power of ultrasonication will be required to achieve optimal dispersion.
- For the rheological experimentation of the NBDF samples, it is recommended to prepare the samples a maximum of one day before, in order to have a valid comparison of results because particles tend to sediment.
- When working with samples of NBDF at high temperatures, it is necessary to change the samples in each experimental repetition, since they deteriorate irreversibly due to received heat. In addition, it is necessary to resort to a mechanism that prevents the evaporation of water.
- For future studies, it is recommended to carry out rheological investigations taking into account the particle size of the sodium bentonite used, in order to analyze the interaction of the carbon particles with the bentonite particles and study their influence on the rheological properties of the fluid.

Chapter 7

Appendix

In the following table, based on the paper "*Carbon allotropes: beyond graphite and diamond*", some allotropic forms of carbon are presented.¹⁶ The table also summarizes the most important properties of each allotrope.

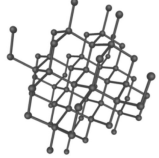
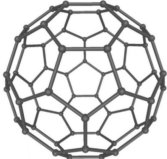
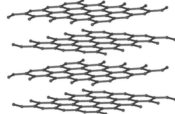
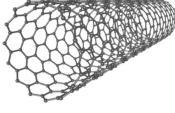
Substance	Properties	Figure
Diamond (sp^3)	Hardness and high thermal conductivity	 (a)
Fullerene (sp^2)	Electronic and optical properties, potential high hardness in composites, superconducting, and high strength.	 (b)
Graphene (sp^2)	Unique electronic properties.	 (c)
Graphite (sp^2)	Anisotropic electronic conductivity, lubricity.	 (d)
Carbon Nanotubes (sp^2)	Electronic properties, high strength	 (e)

Table 7.1: Allotropic forms of element carbon and their properties. Model structures of carbon: (a) diamond, (b) fullerene, (c) graphene, (d) graphite, and (e) carbon nanotubes. The figures were adapted from a model created by Michael Ströck. Source of Table: Reference [16]

Bibliography

- [1] Ismail, A. R.; Sulaiman, W.; Jaafar, M.; Aftab, A.; Razi, A.; Ibutoto, Z. The application of MWCNT to enhance the rheological behavior of drilling fluids at high temperature. *Malaysian Journal of Fundamental and Applied Sciences* **2016**, *12*, 95–98.
- [2] Ismail, A. R.; Rashid, N. M.; Jaafar, M. Z.; Sulaiman, W. R. W.; Buang, N. A. Effect of nanomaterial on the rheology of drilling fluids. *Journal of Applied Sciences* **2014**, *14*, 1192.
- [3] Espinosa, S.; Stalin, C. Estudio y caracterización reológica de fluidos de perforación basados en agua y bentonita sódica natural. B.S. thesis, Universidad de las Fuerzas Armadas ESPE. Carrera de Ingeniería Mecánica., 2017.
- [4] Villarroel Aguirre, L. C. Diseño de un fluido de perforación drill-in compuesto por carbonato de calcio para minimizar el daño en formaciones productoras en el campo Sacha. B.S. thesis, Quito: UCE., 2014.
- [5] Amanullah, M.; AlArfaj, M.; Al-abdullatif, Z. Preliminary Test Results of Nano-based Drilling Fluids for Oil and Gas Field Application. 2011.
- [6] Skalle, P. *Drilling fluid engineering*; Bookboon, 2011.
- [7] Nwaiche, J. Selection and Application of Drilling Fluids. 2015.
- [8] Oltedal, V. M.; Werner, B.; Lund, B.; Saasen, A.; Ytrehus, J. D. Rheological properties of oil based drilling fluids and base oils. 2015.
- [9] Wiliamson, D. Fundamento de los fluidos de perforación. *Oilfield Review* **2013**, *25*, 67–69.
- [10] Luckham, P. F.; Rossi, S. The colloidal and rheological properties of bentonite suspensions. *Advances in colloid and interface science* **1999**, *82*, 43–92.

- [11] Abu-Jdayil, B.; Ghannam, M. The modification of rheological properties of sodium bentonite-water dispersions with low viscosity CMC polymer effect. *Energy Sources, Part A: Recovery, Utilization, and Environmental Effects* **2014**, *36*, 1037–1048.
- [12] Ismail, A.; Aftab, A.; Ibupoto, Z.; Zolkifile, N. The novel approach for the enhancement of rheological properties of water-based drilling fluids by using multi-walled carbon nanotube, nanosilica and glass beads. *Journal of Petroleum Science and Engineering* **2016**, *139*, 264–275.
- [13] Neff, J. M.; McKelvie, S.; Ayers Jr, R. Environmental impacts of synthetic based drilling fluids. **2000**,
- [14] Hughes, B. Drilling fluids reference manual. *Houston, Texas* **2006**,
- [15] Cencel, Y.; Cimbala, J. Fluid mechanics—fundamentals and applications. **2006**,
- [16] Falcao, E. H.; Wudl, F. Carbon allotropes: beyond graphite and diamond. *Journal of Chemical Technology & Biotechnology: International Research in Process, Environmental & Clean Technology* **2007**, *82*, 524–531.
- [17] Eslava, B. Tipos de Hibridación Del Carbono, Grupos Funcionales y Reacciones de Adición en Química Orgánica. **2017**,
- [18] Martín, N. Sobre fullerenos, nanotubos de carbono y grafenos. *Arbor* **2011**, *187*, 115–131.
- [19] Iijima, S. Carbon nanotubes: past, present, and future. *Physica B: Condensed Matter* **2002**, *323*, 1–5.
- [20] Ariza Bachiller, A.; Casas Yaya, J. C. Estado del arte uso de nanotubos de carbono para la mejora de las propiedades en los concretos. B.S. thesis, 2013.
- [21] Backes, C.; Stemmler, I. Absorption Spectroscopy as a Powerful Technique for the Characterization of Single-Walled Carbon Nanotubes.
- [22] Maria, L. Characterizing exfoliated multiwall carbon nanotubes by Scanning Electron Microscopy and Raman Spectroscopy. M.Sc. thesis.
- [23] Hosseini-Ara, R.; Mirdamadi, H.; Khademyzadeh, H.; Salimi, H. Thermal effect on dynamic stability of single-walled Carbon Nanotubes in low and high temperatures based on Nonlocal shell theory. 2013.
- [24] Jorio, A.; Dresselhaus, G.; Dresselhaus, M. S. *Carbon nanotubes: advanced topics in the synthesis, structure, properties and applications*; Springer Science & Business Media, 2007; Vol. 111.

- [25] Wang, P.; Xiang, R.; Maruyama, S. Thermal Conductivity of Carbon Nanotubes and Assemblies. **2018**,
- [26] Al-Jammal, N.; Juzsakova, T. Review on the Effectiveness of Adsorbent Materials in Oil Spills Clean Up. *Sea* **2017**, *25*, 36.
- [27] Chen, C.; Zhang, Y. *Nanowelded carbon nanotubes: From field-effect transistors to solar microcells*; Springer Science & Business Media, 2009.
- [28] Harris, P. J. Carbon nanotubes and related structures: new materials for the twenty-first century. 2004.
- [29] Choi, J.; Zhang, Y. Single, Double, MultiWall Carbon Nanotube Properties and Applications. *Aldrich Materials Science, Sigma-Aldrich, LLC, accessed Aug* **2016**, *2*, 2017.
- [30] Chen, J.; Hamon, M. A.; Hu, H.; Chen, Y.; Rao, A. M.; Eklund, P. C.; Haddon, R. C. Solution properties of single-walled carbon nanotubes. *Science* **1998**, *282*, 95–98.
- [31] Mittal, V. *Polymer nanocomposite coatings*; CRC Press, 2013.
- [32] Nadeem, S.; Khan, A.; Hussain, S. Model based study of SWCNT and MWCNT thermal conductivities effect on the heat transfer due to the oscillating wall conditions. *International Journal of Hydrogen Energy* **2017**, *42*, 28945–28957.
- [33] Kamel, M. S.; Syeal, R. A.; Abdulhussein, A. A. Heat transfer enhancement using nanofluids: a review of the recent literature. *American Journal of Nano Research and Applications* **2016**, *4*, 1–5.
- [34] Wong, K. V.; De Leon, O. Applications of nanofluids: current and future. *Advances in mechanical engineering* **2010**, *2*, 519659.
- [35] Timofeeva, E. V.; Gavrilov, A. N.; McCloskey, J. M.; Tolmachev, Y. V.; Sprunt, S.; Lopatina, L. M.; Selinger, J. V. Thermal conductivity and particle agglomeration in alumina nanofluids: experiment and theory. *Physical Review E* **2007**, *76*, 061203.
- [36] Elias, M.; Miqdad, M.; Mahbulul, I.; Saidur, R.; Kamalisarvestani, M.; Sohel, M.; Hepbasli, A.; Rahim, N.; Amalina, M. Effect of nanoparticle shape on the heat transfer and thermodynamic performance of a shell and tube heat exchanger. *International Communications in Heat and Mass Transfer* **2013**, *44*, 93–99.
- [37] Mahbulul, I.; Saidur, R.; Amalina, M.; Elcioglu, E.; Okutucu-Ozyurt, T. Effective ultrasonication process for better colloidal dispersion of nanofluid. *Ultrasonics sonochemistry* **2015**, *26*, 361–369.

- [38] Mahbulul, I.; Chong, T. H.; Khaleduzzaman, S.; Shahrul, I.; Saidur, R.; Long, B.; Amalina, M. Effect of ultrasonication duration on colloidal structure and viscosity of alumina–water nanofluid. *Industrial & Engineering Chemistry Research* **2014**, *53*, 6677–6684.
- [39] Njuguna, J.; Vanli, O. A.; Liang, R. A review of spectral methods for dispersion characterization of carbon nanotubes in aqueous suspensions. *Journal of Spectroscopy* **2015**, *2015*.
- [40] Khopkar, S. M. *Basic concepts of analytical chemistry*; New Age International, 1998.
- [41] Brunatti, C.; Martín, A. Introducción a la espectroscopía de absorción molecular ultravioleta, visible e infrarrojo cercano. *Recuperado el* **2010**, *24*.
- [42] Jiang, L.; Gao, L.; Sun, J. Production of aqueous colloidal dispersions of carbon nanotubes. *Journal of colloid and interface science* **2003**, *260*, 89–94.
- [43] Kharissova, O. V.; Kharisov, B. I. *Solubilization and dispersion of carbon nanotubes*; Springer, 2017; Vol. 250.
- [44] Perkampus, H.-H. *UV-VIS Spectroscopy and its Applications*; Springer Science & Business Media, 2013.
- [45] Sosa, I. A.; Sánchez, J. L. L. Espectrofotometría de Absorción. M.Sc. thesis, Universidad Nacional Autónoma de México. Instituto de Biotecnología, 2004.
- [46] Yu, J.; Grossiord, N.; Koning, C. E.; Loos, J. Controlling the dispersion of multi-wall carbon nanotubes in aqueous surfactant solution. *Carbon* **2007**, *45*, 618–623.
- [47] Westcott, C. *pH measurements*; Elsevier, 2012.
- [48] McMurry, J.; Ballantine, D. S.; Hoeger, C. A.; Peterson, V. E.; Castellion, M. *Fundamentals of general, organic, and biological chemistry*; Pearson Education, 2010.
- [49] Barnes, H. A.; Hutton, J. F.; Walters, K. *An introduction to rheology*; Elsevier, 1989.
- [50] Yadav, S.; Shire, S. J.; Kalonia, D. S. Factors affecting the viscosity in high concentration solutions of different monoclonal antibodies. *Journal of pharmaceutical sciences* **2010**, *99*, 4812–4829.
- [51] The Discovery Hybrid Rheometer. <https://www.tainstruments.com/dhr-2-2/?lang=es>, Accessed: 2019-04-21.

-
- [52] Hielscher, T. Ultrasonic Production of Nano-Size Dispersions and Emulsions. *European Nano Systems 2005, Paris, France, 14-16 December 2005* **2007**,
- [53] Darley, H. C.; Gray, G. R. *Composition and properties of drilling and completion fluids*; Gulf Professional Publishing, 1988.
- [54] Schramm, G. *A practical approach to rheology and rheometry*; Haake Karlsruhe, 1994.
- [55] Goyal, M. *Fluid Mechanics and Hydraulic Machines*; 2015.